Structure Formation

Dr Adrian Jenkins

Institute for Computational Cosmology
Durham University

Talk plan

- Introduction: Structure Formation in ΛCDM Universes
- The internal structure of dark matter halos
- Predictions for annihilation radiation
- Phase space structure in the local dark matter distribution
- Summary

The CMB

1992

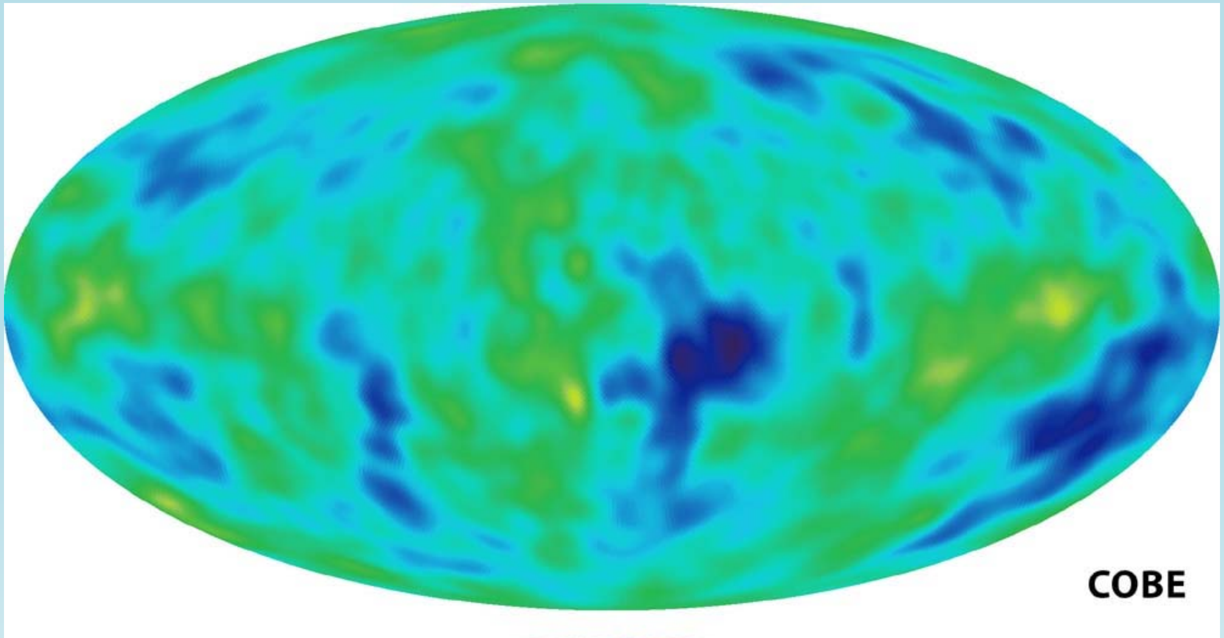

The cosmic microwave background radiation (CMB) provides a window to the universe at t~3x10^5 yrs
In 1992 COBE discovered temperature fluctuations ($\Delta T/T \sim 10^{-5}$) consistent with inflation predictions

The CMB

1992

2003

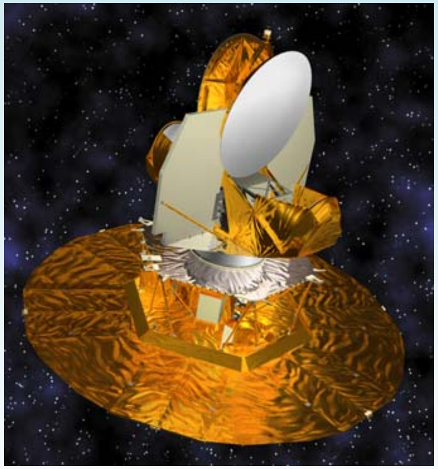

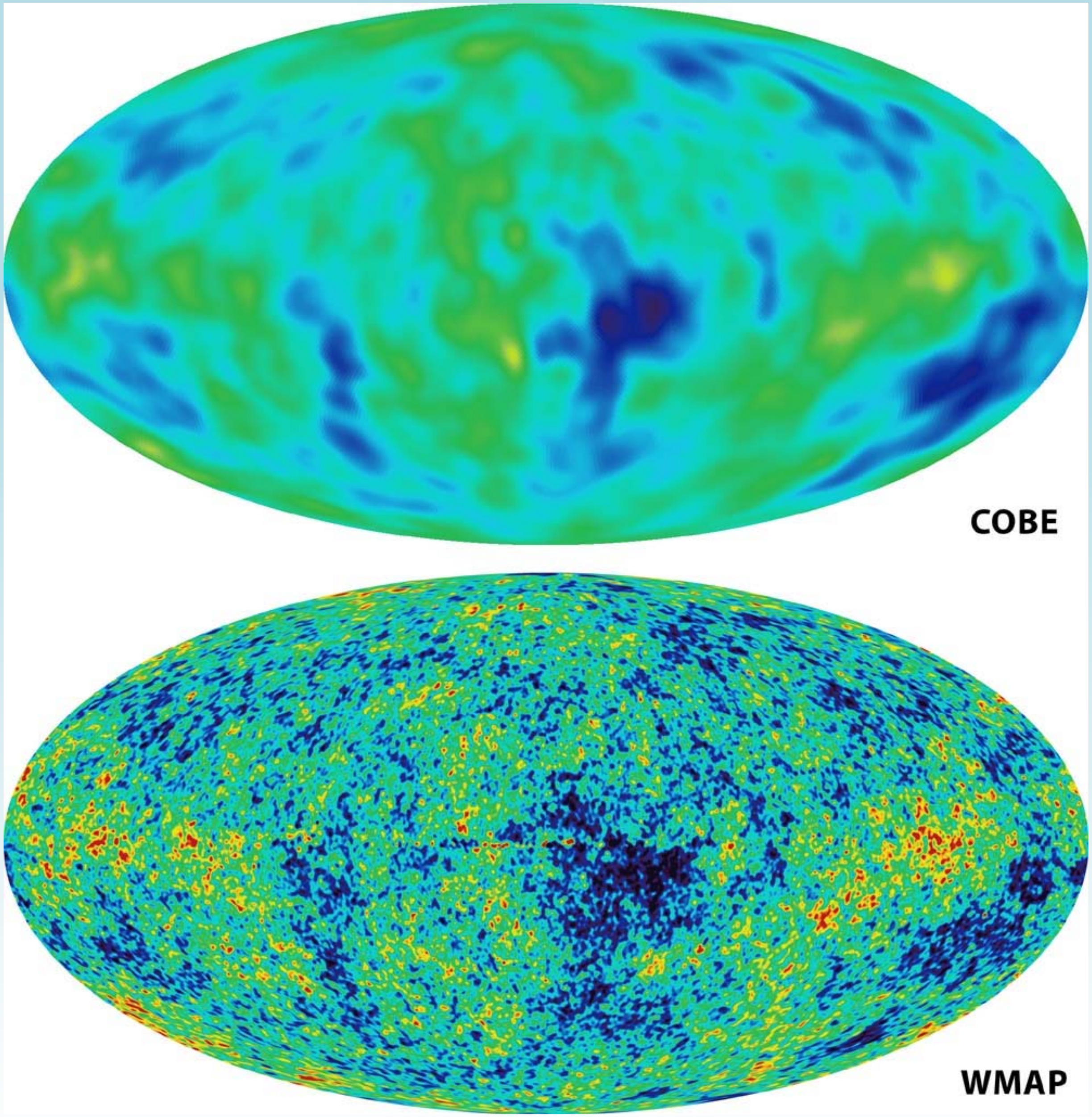

The Emergence of the Cosmic Initial Conditions

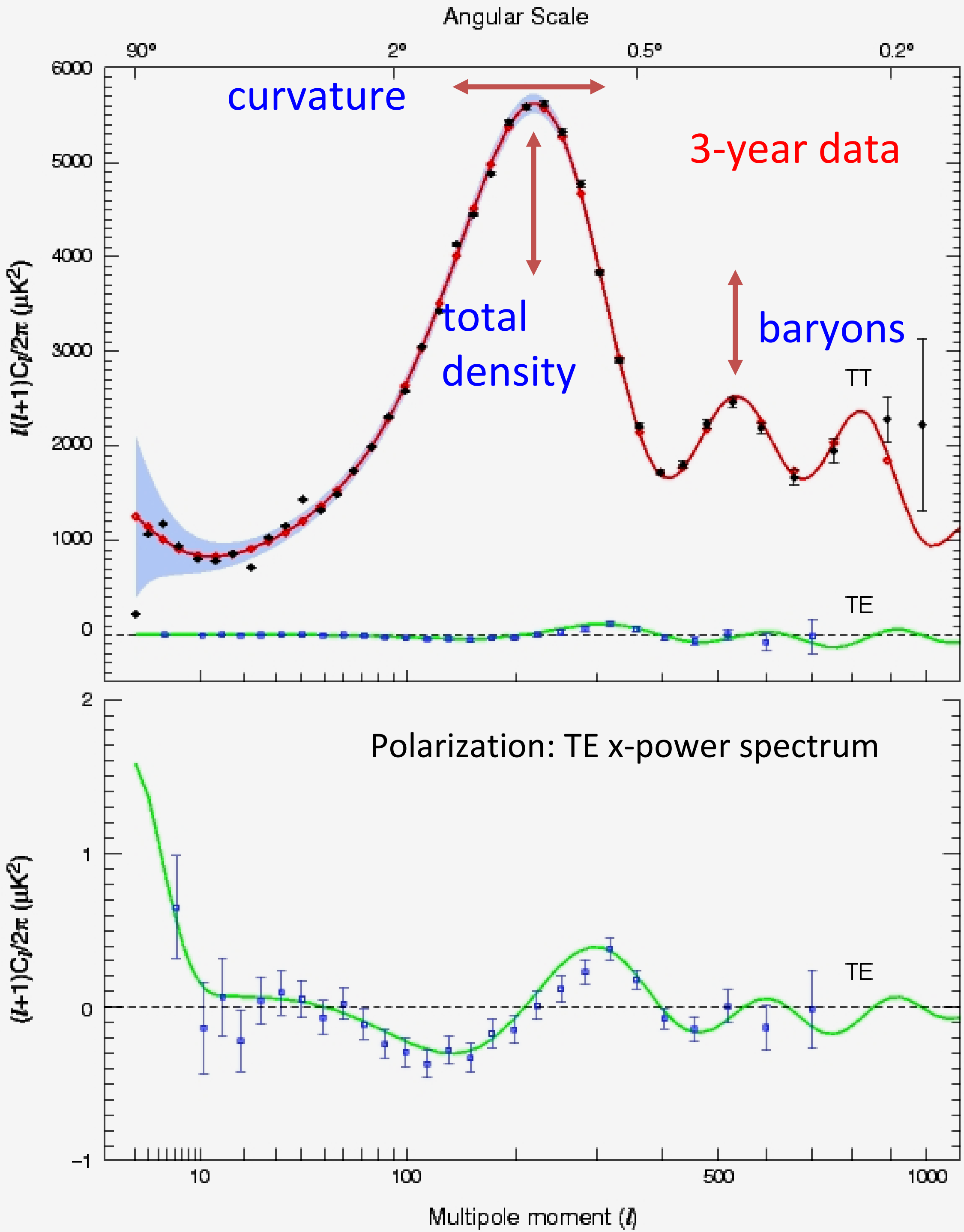

$> 10^5$ independent $\sim 5\sigma$ measurements of T are fit by an *a priori* model: ΛCDM

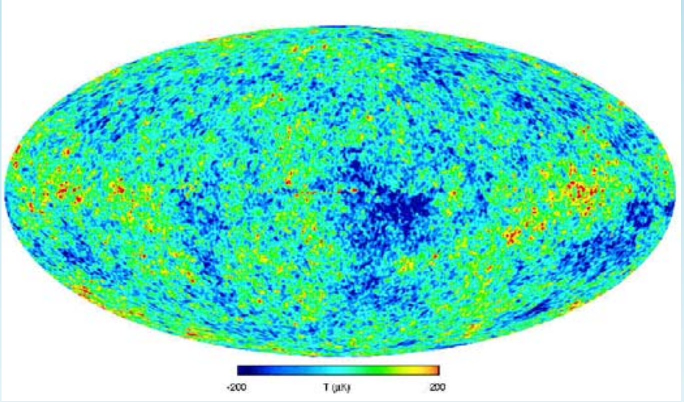

T-E x-corr →Adiabatic fluctns


2003: The 2dF Galaxy Redshift Survey
221,000 redshifts

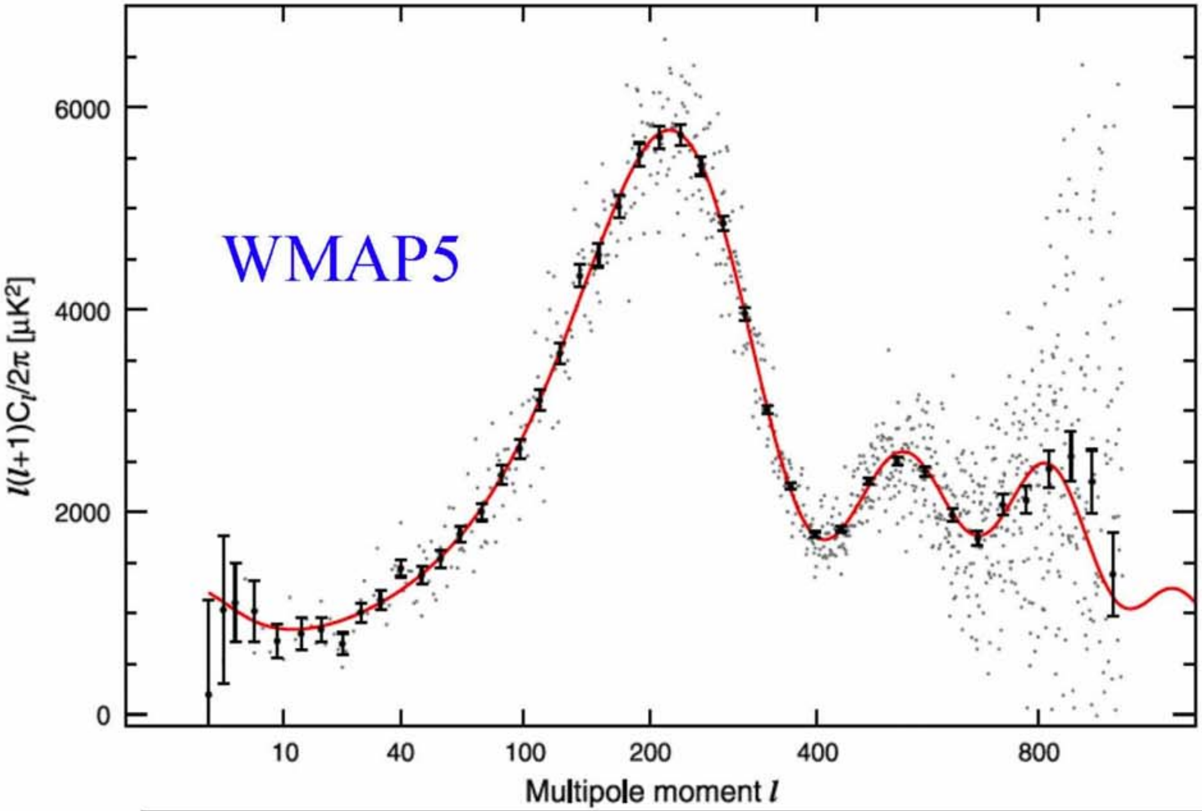

2df galaxy survey

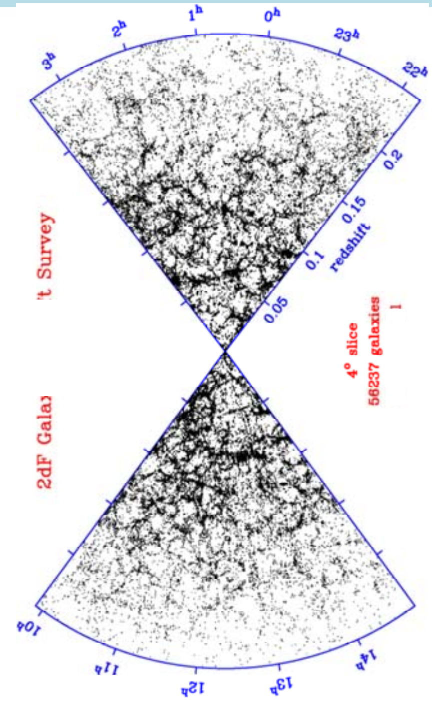

parameter	symbol	WMAP-5 alone	WMAP-5 + BAO + SNe	comment
CMB temperature	T_{CMB}	2.728 ± 0.004 K	–	from (Fixsen *et al.* 1996)
total matter density	Ω_{tot}	$1.099 \, ^{+0.100}_{-0.085}$	1.0052 ± 0.0064	
matter density	Ω_{m0}	0.258 ± 0.03	0.279 ± 0.015	assuming spatial flatness
baryon density	Ω_{b0}	0.0441 ± 0.0030	0.0462 ± 0.0015	here and below
cosmological constant	$\Omega_{\Lambda 0}$	0.742 ± 0.03	0.721 ± 0.015	
Hubble constant	h	$0.719 \, ^{+0.026}_{-0.027}$	0.701 ± 0.013	
power-spectrum normalisation	σ_8	0.796 ± 0.036	0.817 ± 0.026	
age of the Universe in Gyr	t_0	13.69 ± 0.13	13.73 ± 0.12	
decoupling redshift	z_{dec}	1087.9 ± 1.2	1088.2 ± 1.1	
reionisation optical depth	τ	0.087 ± 0.017	0.084 ± 0.016	
spectral index	n_{s}	$0.963 \, ^{+0.014}_{-0.015}$	$0.960 \, ^{+0.014}_{-0.013}$	

The cosmic power spectrum

CMB:

- Convert angular separation to distance (and k) assuming flat geometry
- Extrapolate to z=0 using linear theory

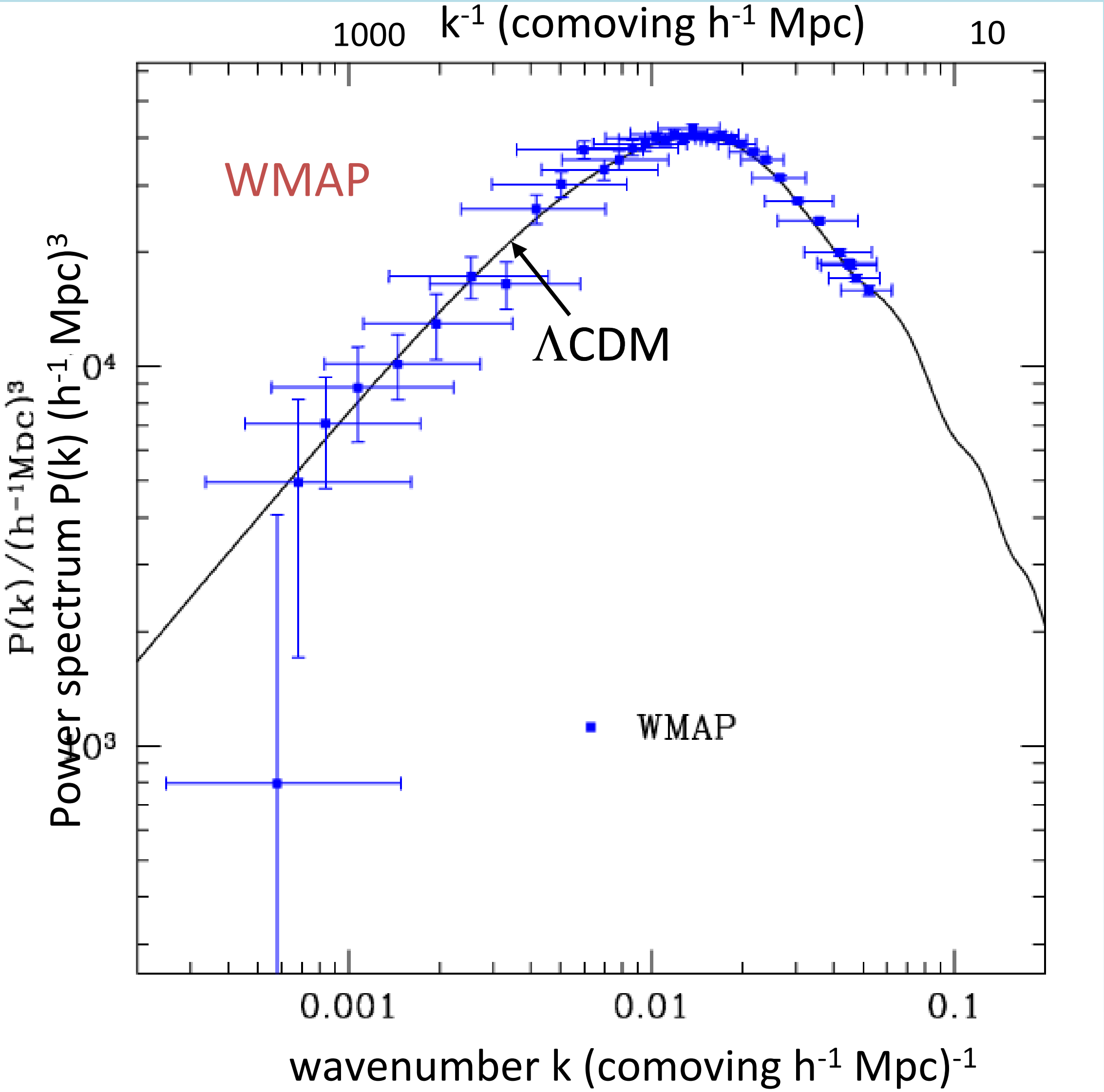

The cosmic power spectrum: from the CMB to the 2dFGRS

CMB:

- Convert angular separation to distance (and k) assuming flat geometry
- Extrapolate to z=0 using linear theory

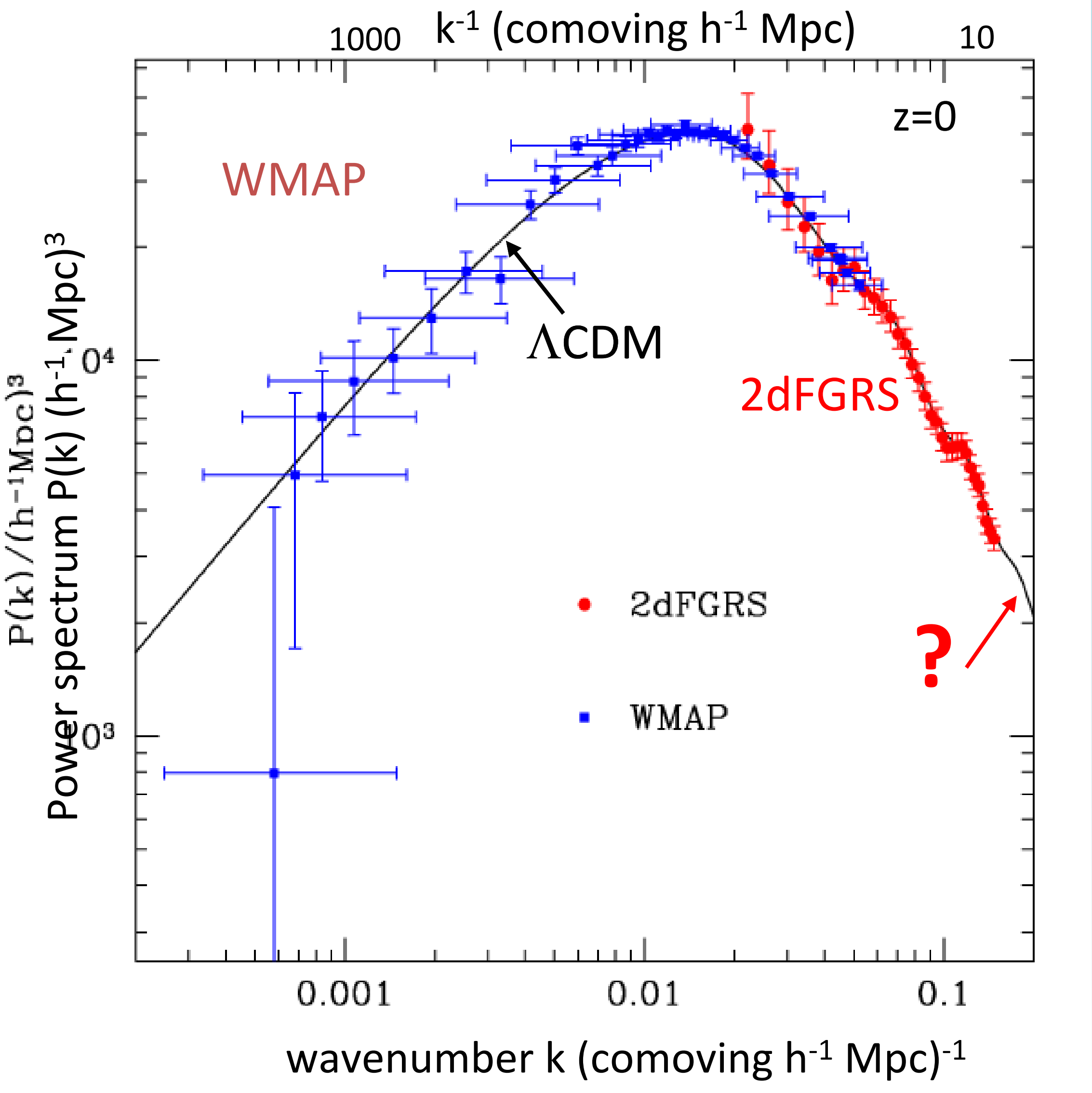

$\Longrightarrow$ ΛCDM provides an excellent description of mass power spectrum from 10-1000 Mpc

Sanchez et al 06

The cold dark matter power spectrum

The linear power spectrum ("power per octave")

Assumes a 100GeV wimp
Green et al '04

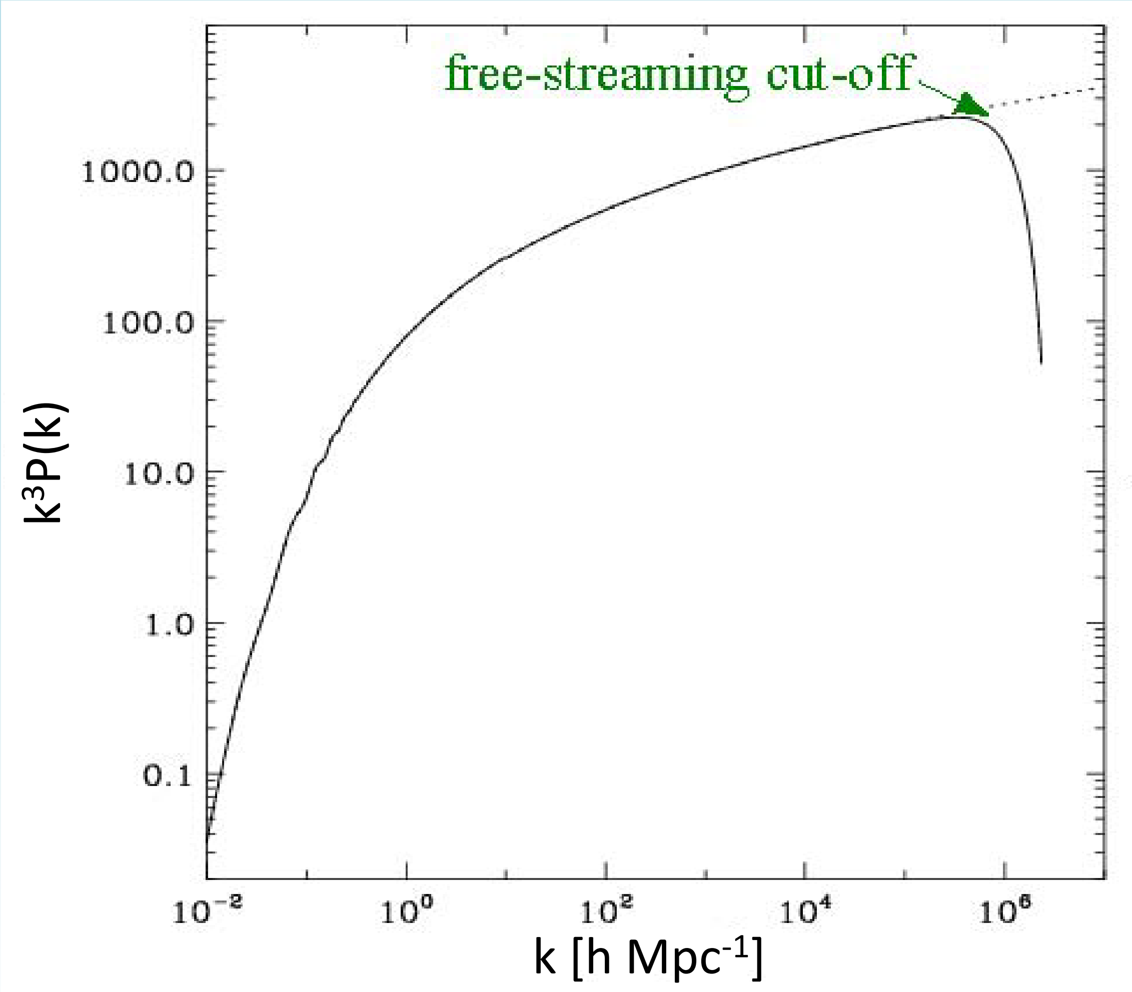

Talk plan

- Introduction: Structure Formation in ΛCDM Universes
- The internal structure of dark matter halos
- Predictions for annihilation radiation
- Phase space structure in the local dark matter distribution
- Summary

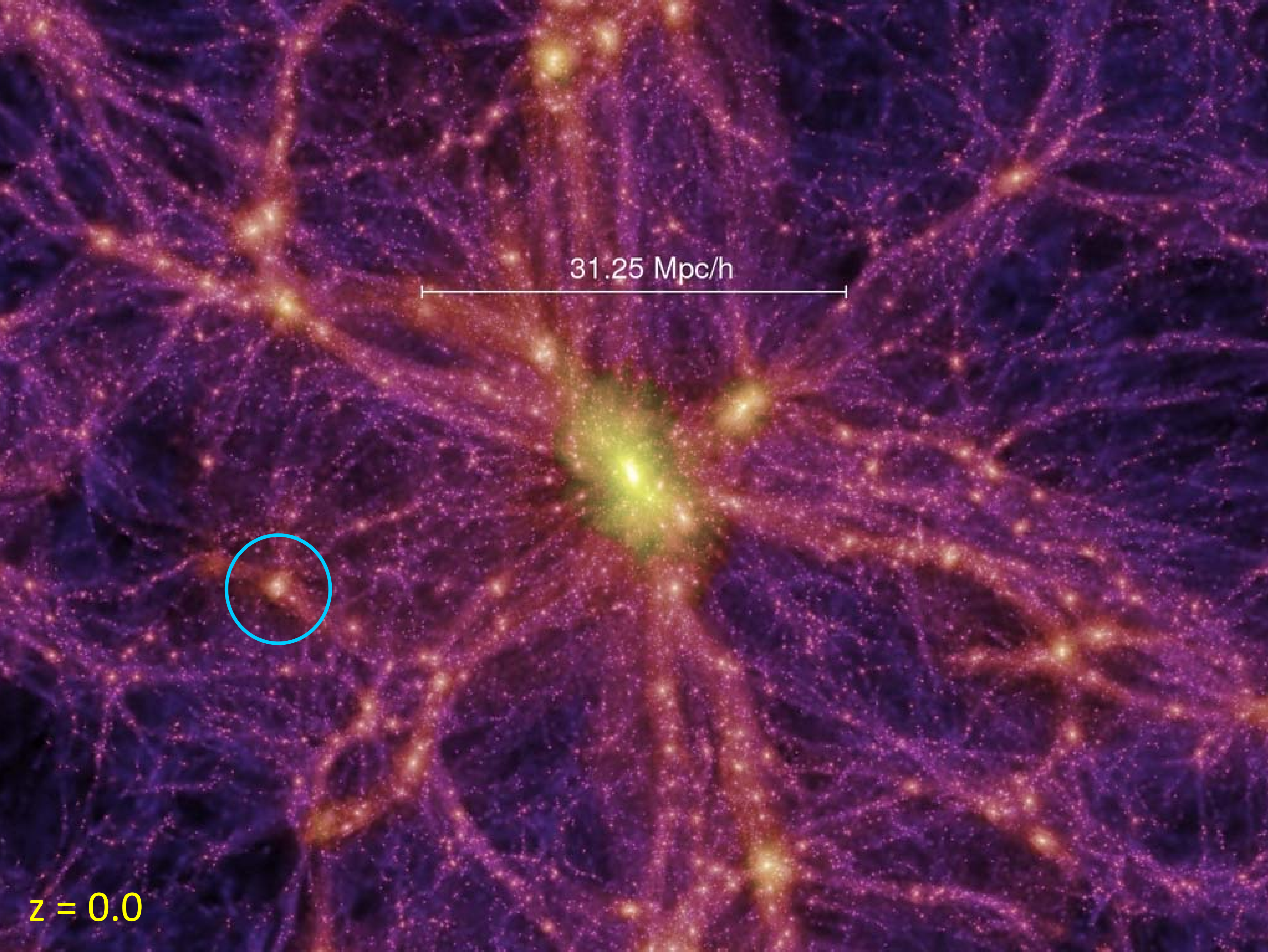
31.25 Mpc/h
z = 0.0


z = 0.1
A galactic dark matter halo
1.1 billion particles inside r_{vir}
Springel, Wang, Volgensberger, Ludlow, Jenkins, Helmi, Navarro, Frenk & White '08
Aq-A-1 simulation

Aquarius Papers

- A Blueprint for detecting supersymmetric dark matter in the Galactic halo, Nature, 456, 73
  Springel, White, Frenk, Navarro, Jenkins, Vogelsberger, Wang, Ludlow, Helmi
- The Aquarius Project: Abundance and structure of dark matter subhalos, MNRAS, 2008, 391, 1685
  Springel, Wang, Vogelsberger, Ludlow, Jenkins, Helmi, Navarro, Frenk, White
- The Diversity and Similarity of Cold Dark Matter Halos, MNRAS (submitted), arXiv0810.1522
  Navarro, Ludlow, Springel, Wang, Vogelsberger, White, Jenkins, Frenk, Helmi
- The phase space-structure in the local dark matter distribution and its signature in direct detection experiments, MNRAS, Vogelsberger, Helmi, Springel, White, Wang, Frenk, Jenkins, Ludlow, Navarro, MNRAS, 395, 797.

The Aquarius Project

- Virgo Consortium project.

- Supercomputer Simulations run at (LRZ, RZG, MPA), COSMA (Durham), STELLA (LOFAR correlator)

- Starting point was a parent ΛCDM simulation – 100 Mpc/h on a side with the same cosmological parameters as the Millennium simulation.

The six aquarius halos.

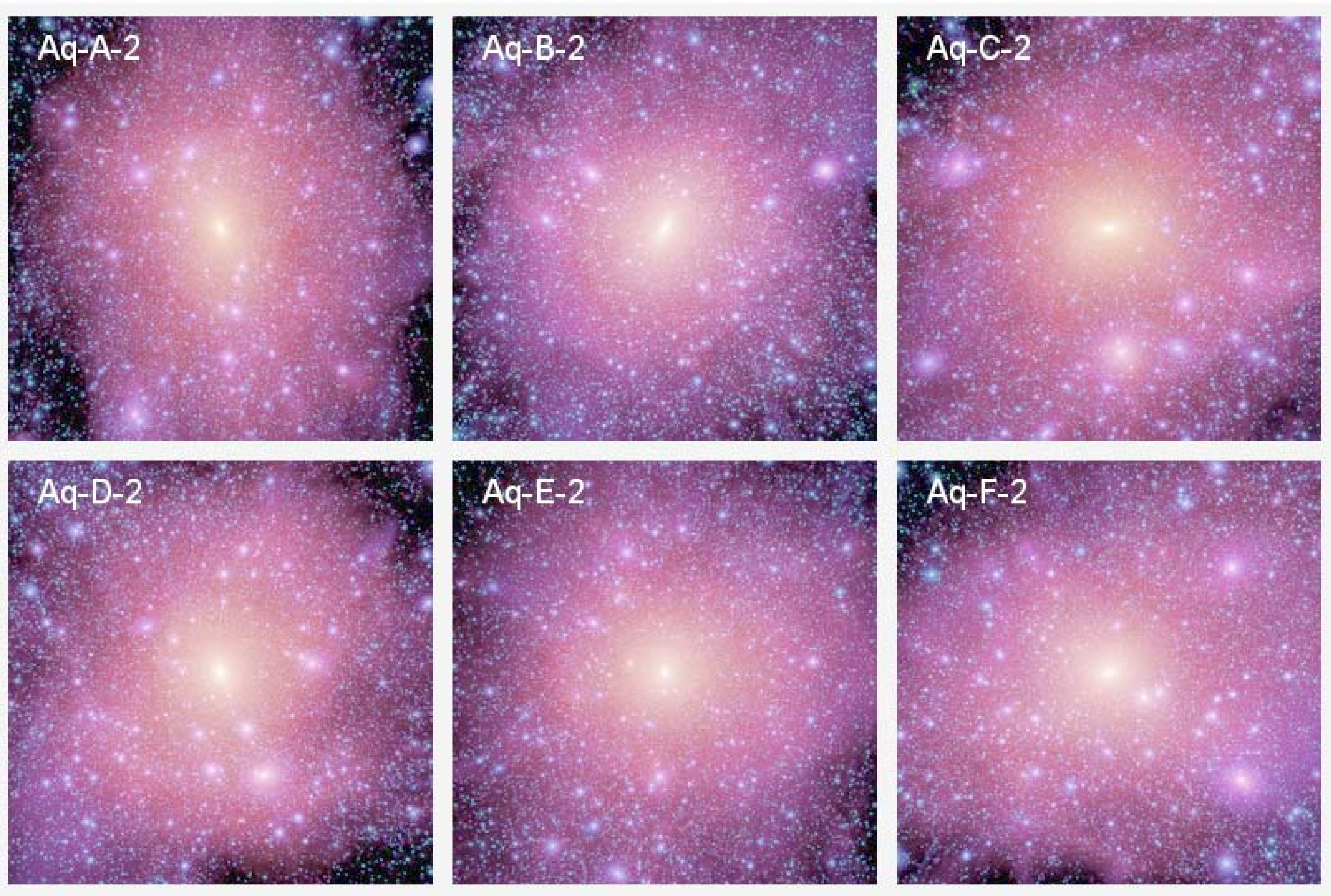

Aquarius Sample

Name	m_p [$M_\odot$]	ϵ [pc]	N_{hr}	N_{lr}	M_{200} [$M_\odot$]	r_{200} [kpc]	M_{50} [$M_\odot$]	r_{50} [kpc]	N_{50}
Aq-A-1	1.712×10^3	20.5	4,252,607,000	144,979,154	1.839×10^{12}	245.76	2.523×10^{12}	433.48	1,473,568,512
Aq-A-2	1.370×10^4	65.8	531,570,000	75,296,170	1.842×10^{12}	245.88	2.524×10^{12}	433.52	184,243,536
Aq-A-3	4.911×10^4	120.5	148,285,000	20,035,279	1.836×10^{12}	245.64	2.524×10^{12}	433.50	51,391,468
Aq-A-4	3.929×10^5	342.5	18,535,972	634,793	1.838×10^{12}	245.70	2.524×10^{12}	433.52	6,424,399
Aq-A-5	3.143×10^6	684.9	2,316,893	634,793	1.853×10^{12}	246.37	2.541×10^{12}	434.50	808,479
Aq-B-2	6.447×10^3	65.8	658,815,010	80,487,598	8.194×10^{11}	187.70	1.045×10^{12}	323.12	162,084,992
Aq-B-4	2.242×10^5	342.5	18,949,101	648,874	8.345×10^{11}	188.85	1.050×10^{12}	323.60	4,683,037
Aq-C-2	1.399×10^4	65.8	612,602,795	78,634,854	1.774×10^{12}	242.82	2.248×10^{12}	417.09	160,630,624
Aq-C-4	3.213×10^5	342.5	26,679,146	613,141	1.793×10^{12}	243.68	2.285×10^{12}	419.36	7,110,775
Aq-D-2	1.397×10^4	65.8	391,881,102	79,615,274	1.774×10^{12}	242.85	2.519×10^{12}	433.21	180,230,512
Aq-D-4	2.677×10^5	342.4	20,455,156	625,272	1.791×10^{12}	243.60	2.565×10^{12}	435.85	9,579,672
Aq-E-2	9.593×10^3	65.8	465,905,916	74,119,996	1.185×10^{12}	212.28	1.548×10^{12}	368.30	161,323,676
Aq-E-4	2.604×10^5	342.5	17,159,996	633,106	1.208×10^{12}	213.63	1.558×10^{12}	369.14	5,982,797
Aq-F-2	6.776×10^3	65.8	414,336,000	712,839	1.135×10^{12}	209.21	1.517×10^{12}	365.87	223,901,216
Aq-F-3	2.287×10^4	120.5	122,766,400	712,839	1.101×10^{12}	207.15	1.494×10^{12}	363.98	65,320,572

Comparable simulations

GHALO$_{2,3,4,5}$	Stadel et al 2008	~1.0 billion particles
VLII	Diemand et al 08	~0.4 billion particles
VLI	Diemand et al 07	~0.08 billion particles

The cold dark matter power spectrum

The linear power spectrum ("power per octave")

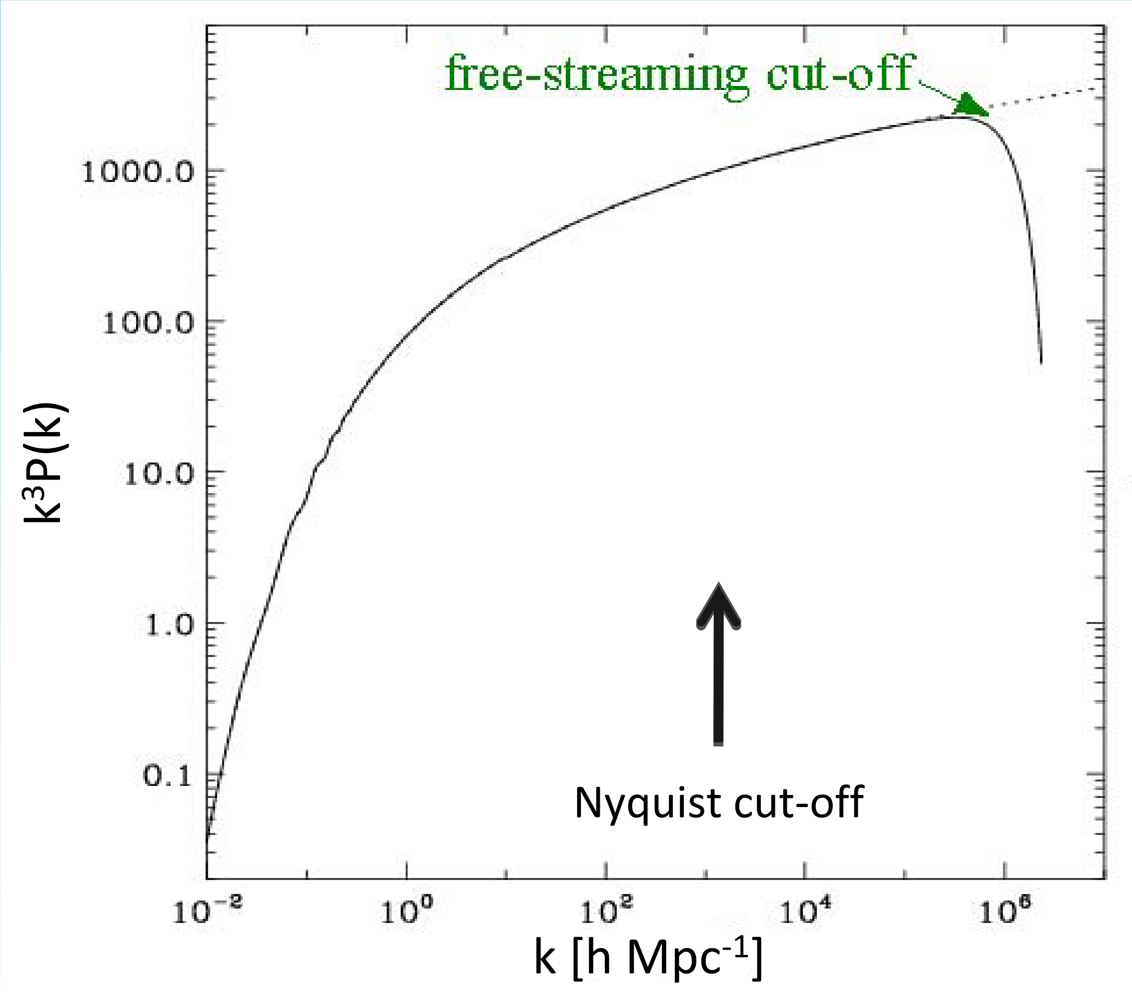

Assumes a 100GeV wimp

Green et al '04


z = 48.4
T = 0.05 Gyr
500 kpc

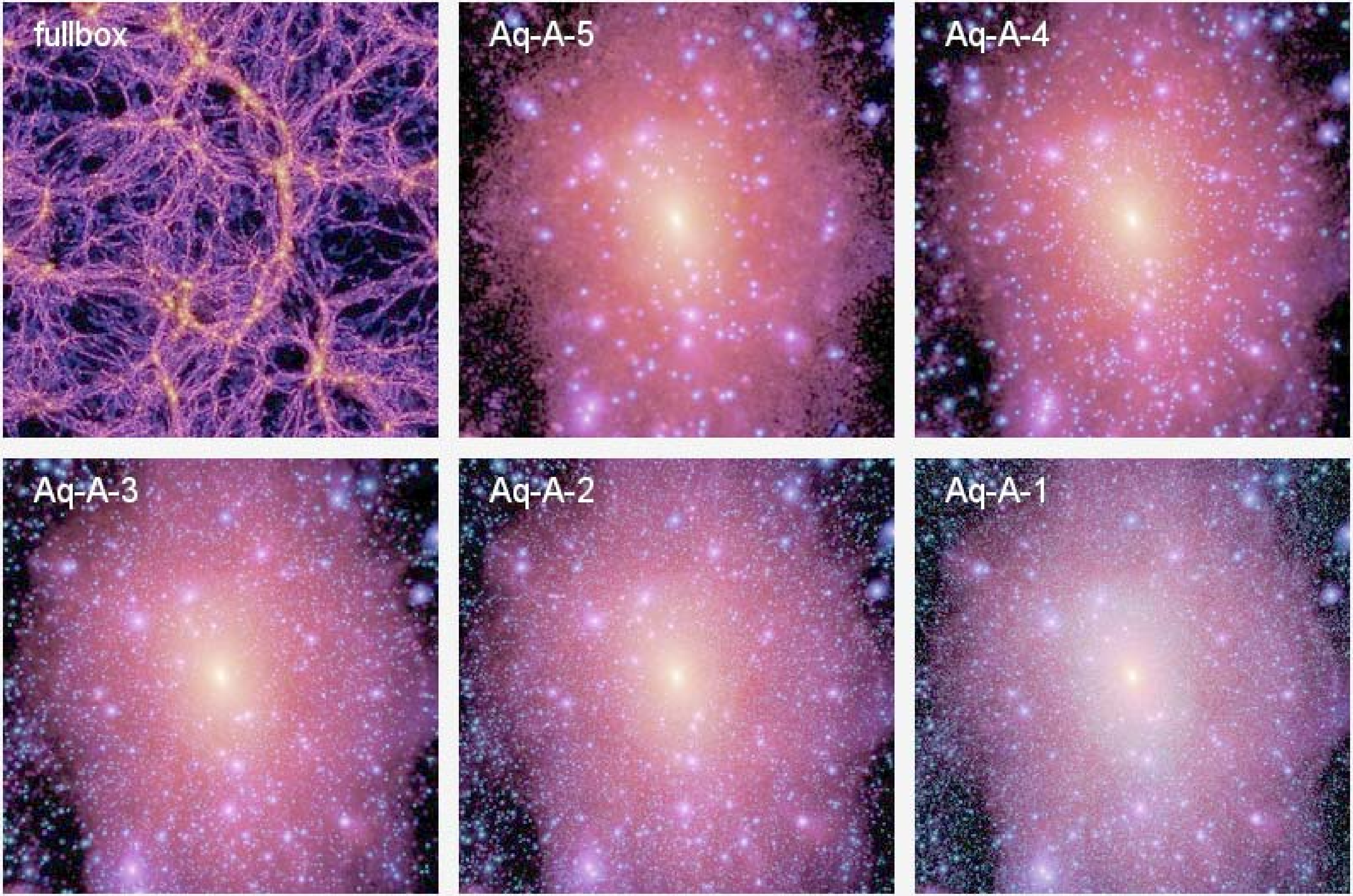
fullbox
Aq-A-5
Aq-A-4
Aq-A-3
Aq-A-2
Aq-A-1

Density profile ρ(r): convergence test

The spherically averaged density profiles show very good convergence, and are approximately fit by a NFW profile

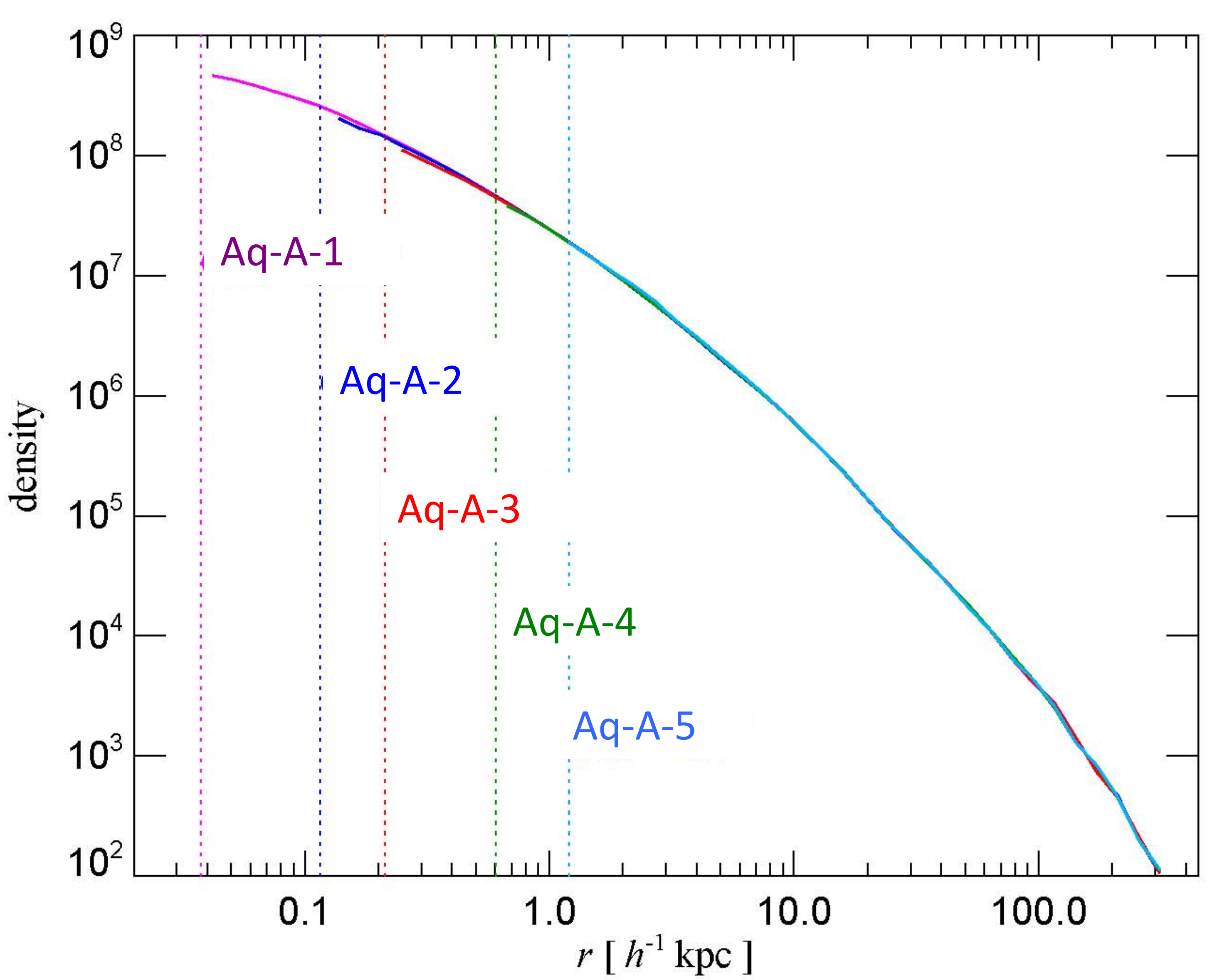

Slope of the density profile

Density profile becomes shallower towards the centre

No obvious convergence to a power law profile
Innermost slope is shallower than -1

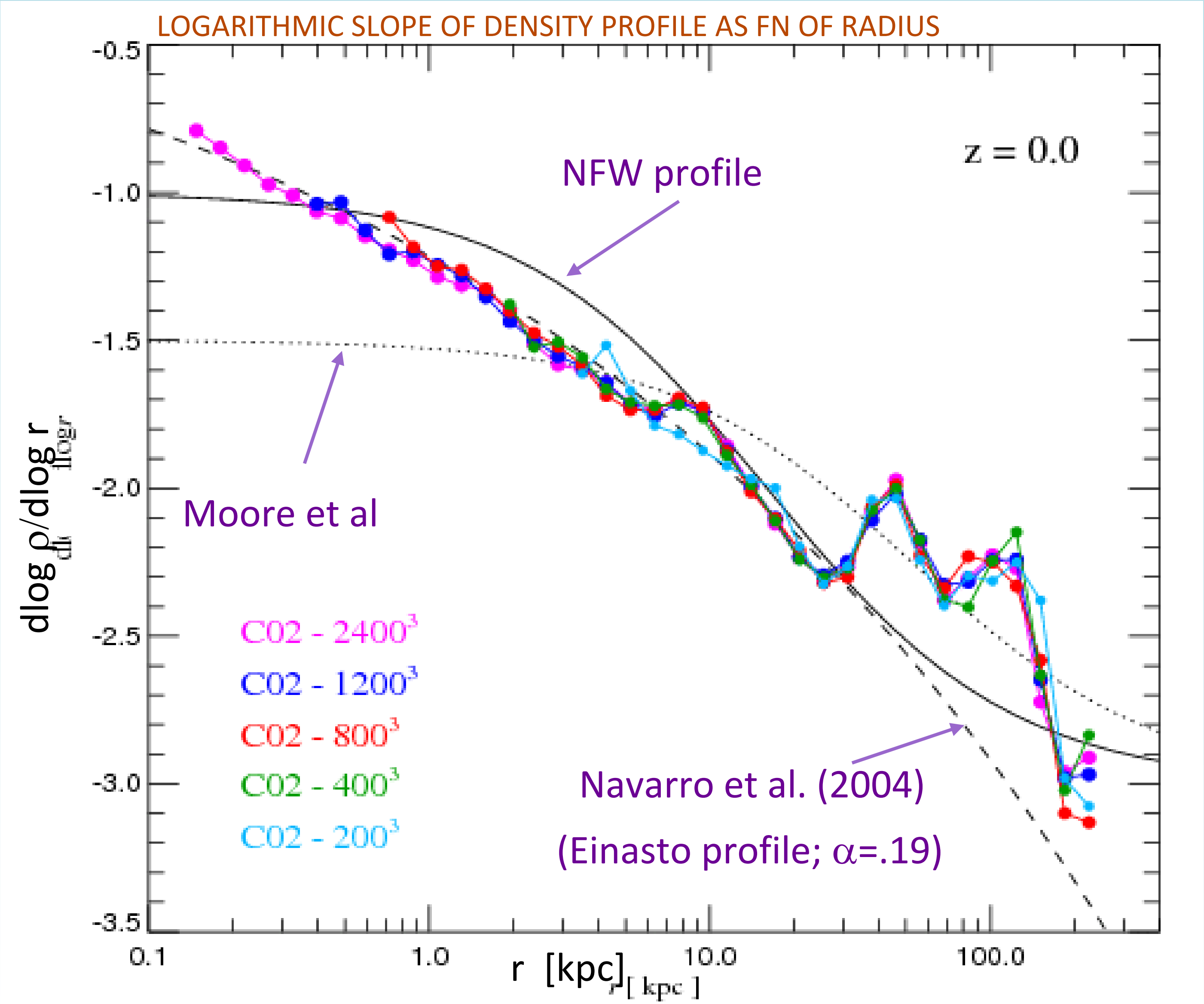

Virgo Consortium 08

Velocity structure: convergence test

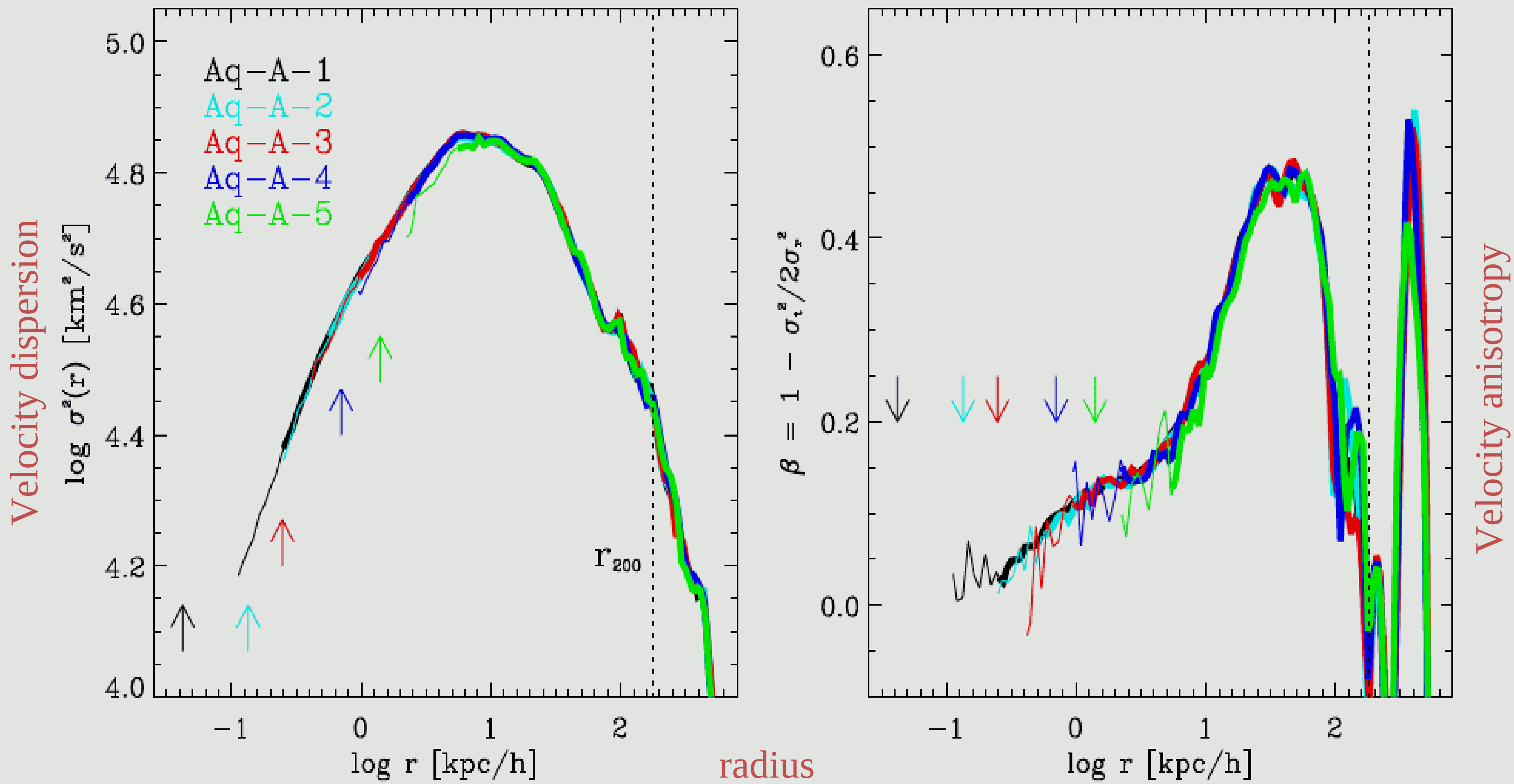

Excellent numerical convergence down to radius where the collisional relaxation time approaches the age of the universe

Virgo Consortium 08

The mass function of substructures

The subhalo mass function is shallower than M^2

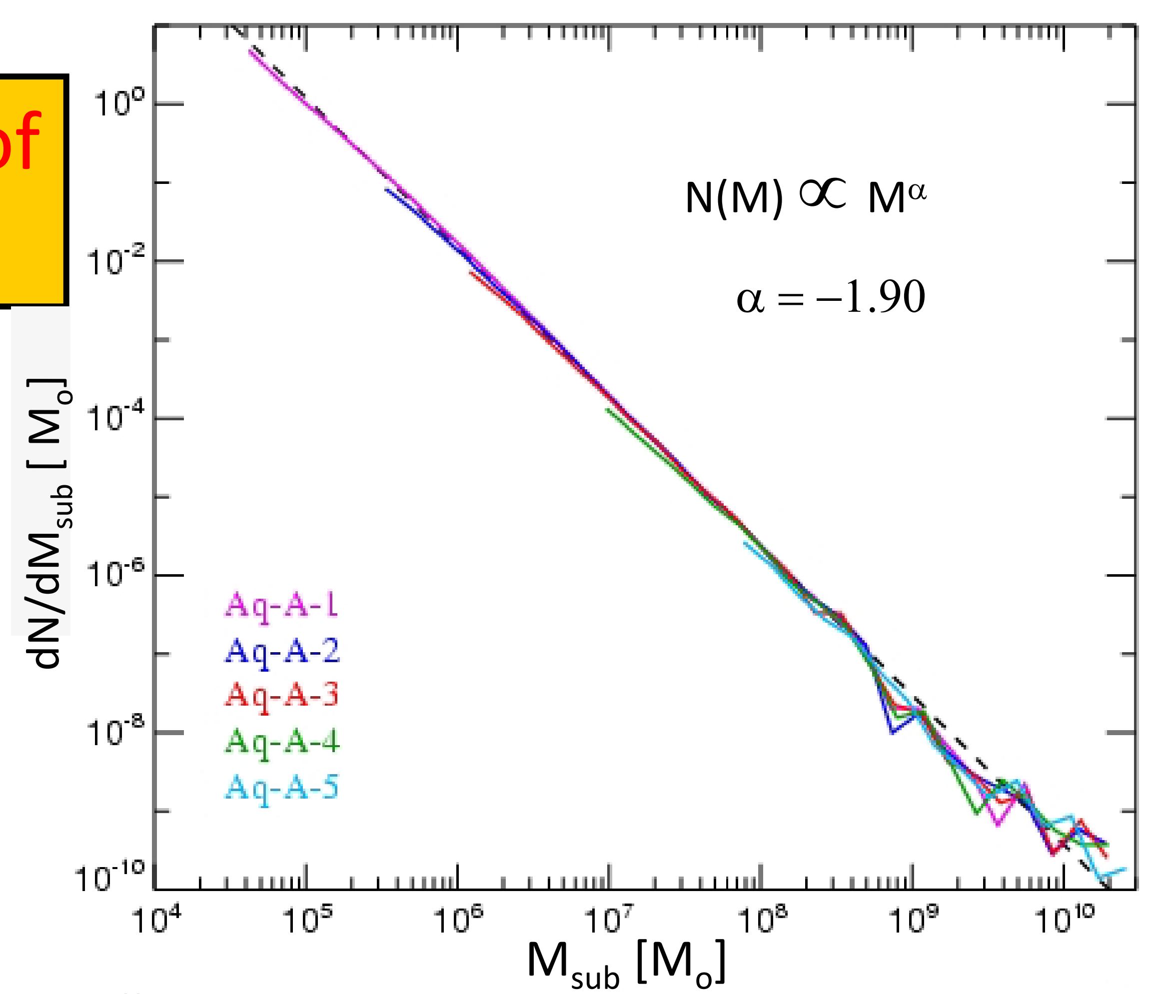

Most of the substructure mass is in the few most massive halos

The total mass in substructures converges slowly as numerical resolution improves.

300,000 subhalos within virialized region in Aq-A-1

Virgo consortium
Springel et al 08

Springel, Wang, Vogelsberger, Ludlow, Jenkins, Helmi, Navarro, Frenk & White '08

The mass function of substructures

The subhalo mass function is shallower than M^2

Most of the substructure mass is in the few most massive halos

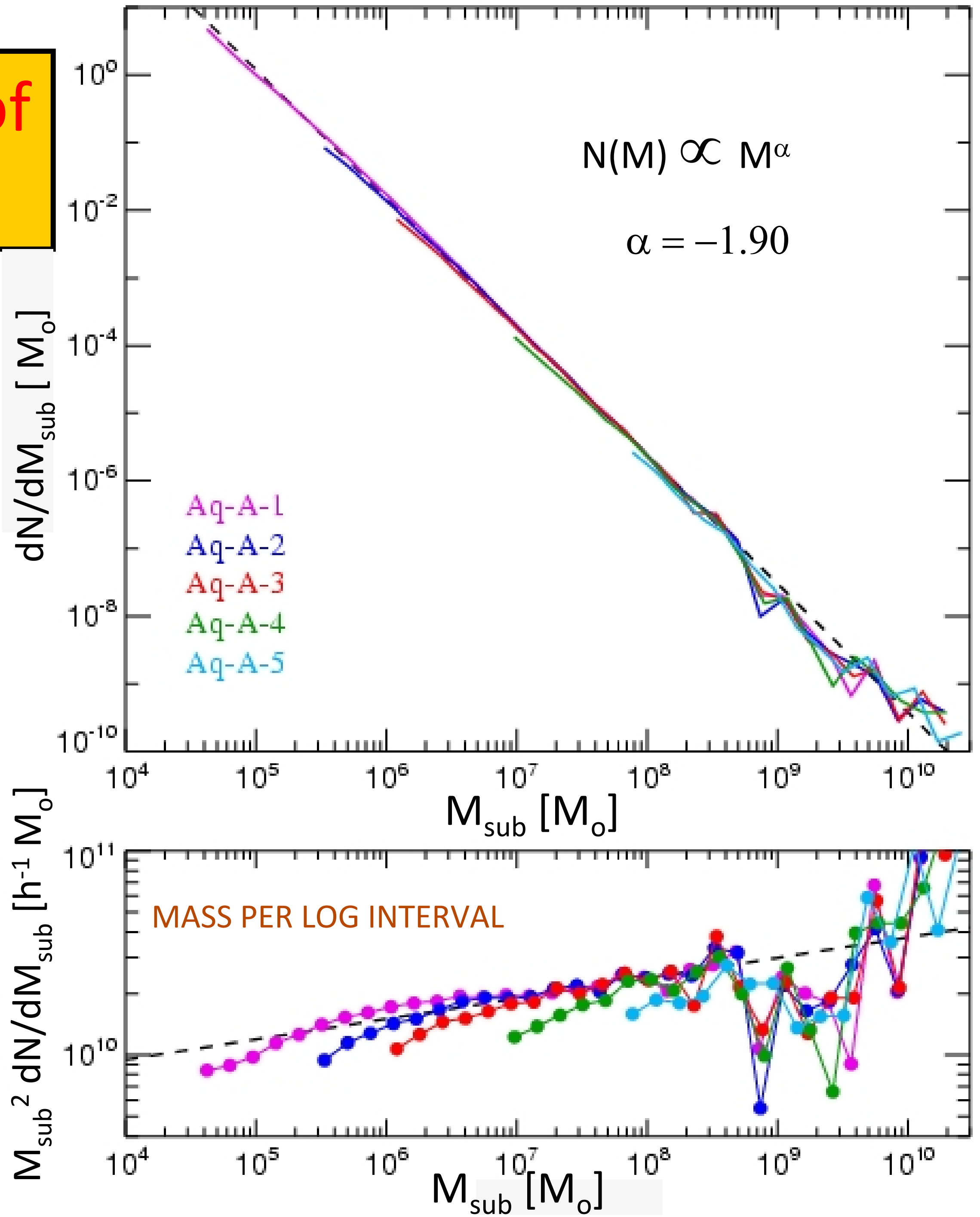

Virgo consortium
Springel et al 08

The substructure circ velocity function

CUMULATIVE NUMBER OF SUBSTRUCTURES AS A FUNCTION OF VMAX,

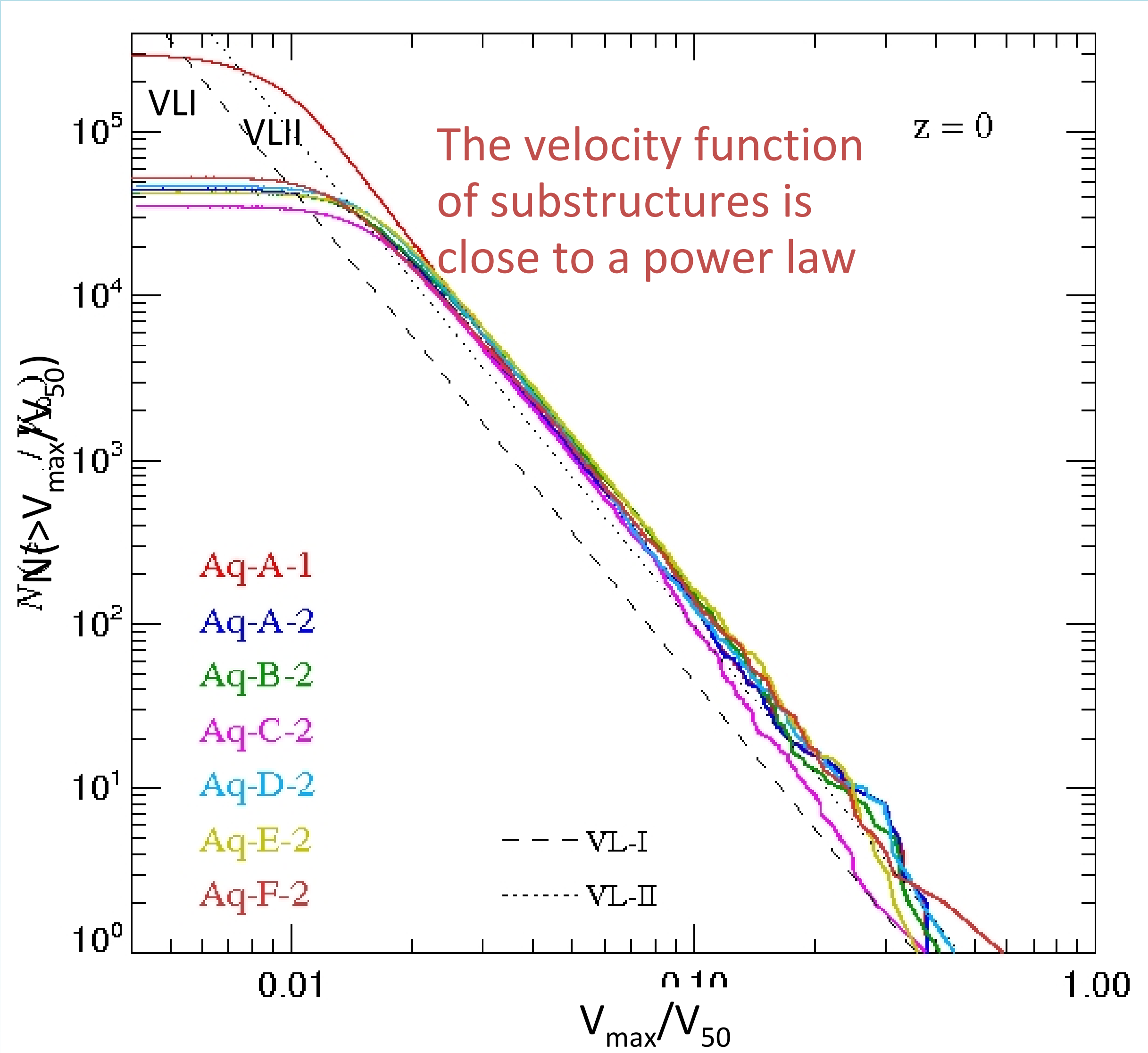

VLII shows similar amounts of substructure to our ensemble.

We find *3 times* as many subhalos as Diemand et al find for VL I, but this due to a fault in the VL I initial conditions.

Halo properties

Name	$V_{\rm max}$ [$\rm km\,s^{-1}$]	$r_{\rm max}$ [kpc]	δ_V	$c^*_{\rm NFW}$	$z_{\rm form}$	$N_{\rm sub}$	$f^{\rm cumul}_{\rm sub}$
Aq-A-1	208.75	28.35	2.035×10^4	16.11	1.93	297791	13.20 %
Aq-A-2	208.49	28.14	2.060×10^4	16.19	1.93	45024	12.16 %
Aq-A-3	209.22	27.88	2.114×10^4	16.35	1.93	13854	11.34 %
Aq-A-4	209.24	28.20	2.067×10^4	16.21	1.93	1960	9.68 %
Aq-A-5	209.17	28.55	2.015×10^4	16.04	1.93	299	8.64 %
Aq-B-2	157.68	40.15	5.788×10^3	9.72	1.39	42537	10.54 %
Aq-B-4	159.03	44.31	4.834×10^3	9.02	1.39	1614	8.26 %
Aq-C-2	222.40	32.47	1.761×10^4	15.21	2.23	35022	7.17 %
Aq-C-4	223.20	33.63	1.654×10^4	14.84	2.23	1972	6.02 %
Aq-D-2	203.20	54.08	5.299×10^3	9.37	1.51	47014	13.06 %
Aq-D-4	204.47	55.76	5.046×10^3	9.18	1.51	3116	10.67 %
Aq-E-2	179.00	55.50	3.904×10^3	8.26	2.26	42725	10.75 %
Aq-E-4	182.68	54.59	4.202×10^3	8.52	2.26	2024	7.53 %
Aq-F-2	169.08	42.67	5.892×10^3	9.79	0.55	52503	13.39 %
Aq-F-3	174.05	43.76	5.937×10^3	9.82	0.55	12950	9.15 %

Talk plan

- Introduction: Structure Formation in ΛCDM Universes
- The internal structure of dark matter halos
- Predictions for annihilation radiation
- Phase space structure in the local dark matter distribution
- Summary

A blueprint for detecting halo CDM

Supersymmetric particles annihilate and lead to production of γ-rays which may be observable by GLAST/FERMI

The production of annihilation radiation at $\boldsymbol{x}$ depends on:

$$\int \rho^2(\boldsymbol{x}) \quad \langle \sigma v \rangle \, dV$$

halo density at $\boldsymbol{x}$ cross-section

$\Longrightarrow$ Theoretical expectation requires knowing $\rho(\boldsymbol{x})$

$\Longrightarrow$ Accurate high resolution N-body simulations of halo formation from CDM initial conditions

A blueprint for detecting halo CDM

To calculate annihilation luminosity need contribution from 4 components:

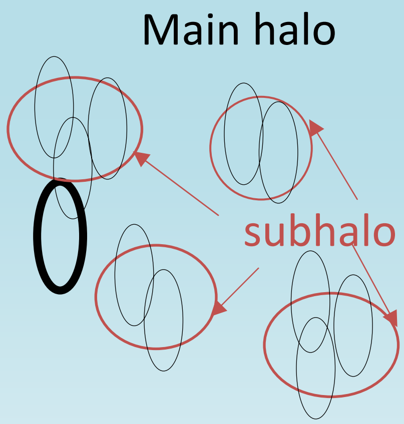

1. Smooth emission from main halo
2. Smooth emission from resolved subhalos
3. Emission from unresolved subhalos in main halo
4. Emission from substructure of subhalos

The subhalo number density profile

- The spatial distribution of subhalos (except for the few most massive ones) is independent of mass
- Most subhalos are at large radii -- subhalos are more effectively destroyed near the centre
- Most Subhalos are far from the Sun – our view of the signal from our own halo is very special.

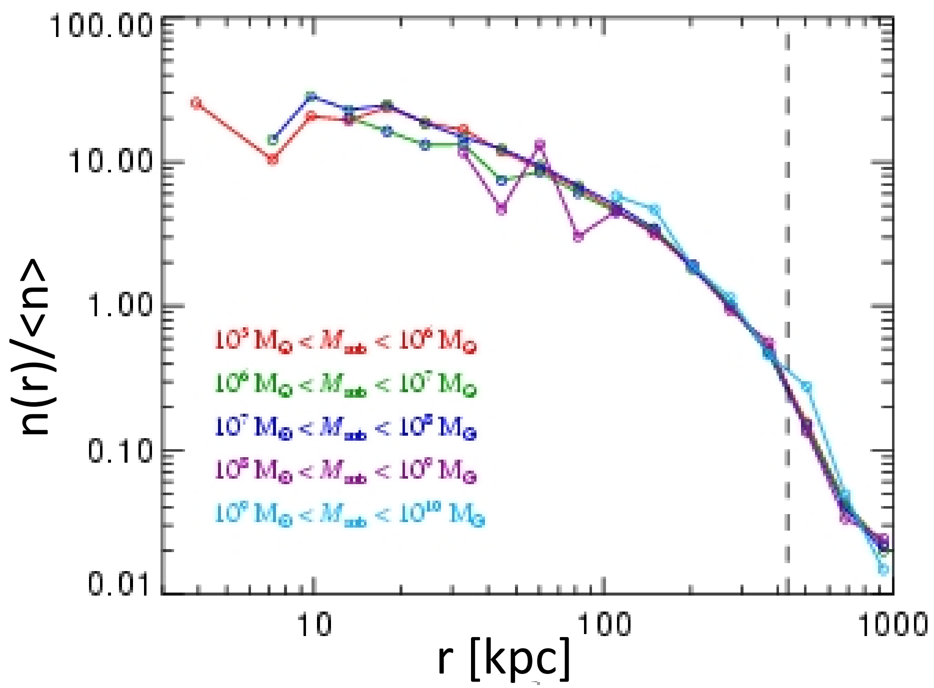

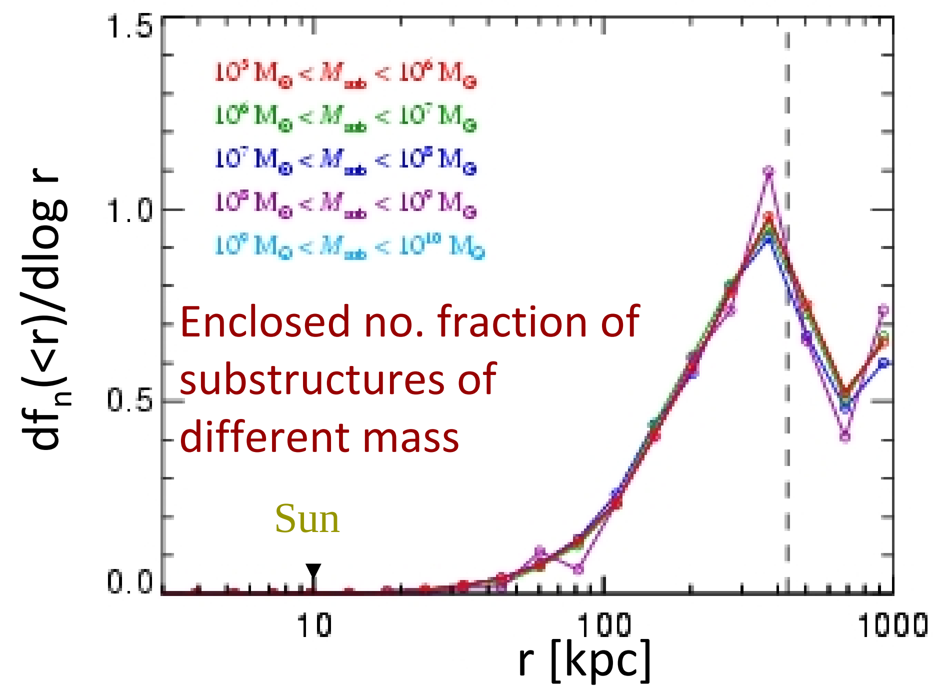

The cold dark matter power spectrum

The linear power spectrum ("power per octave")

Assumes a 100GeV wimp

Green et al '04

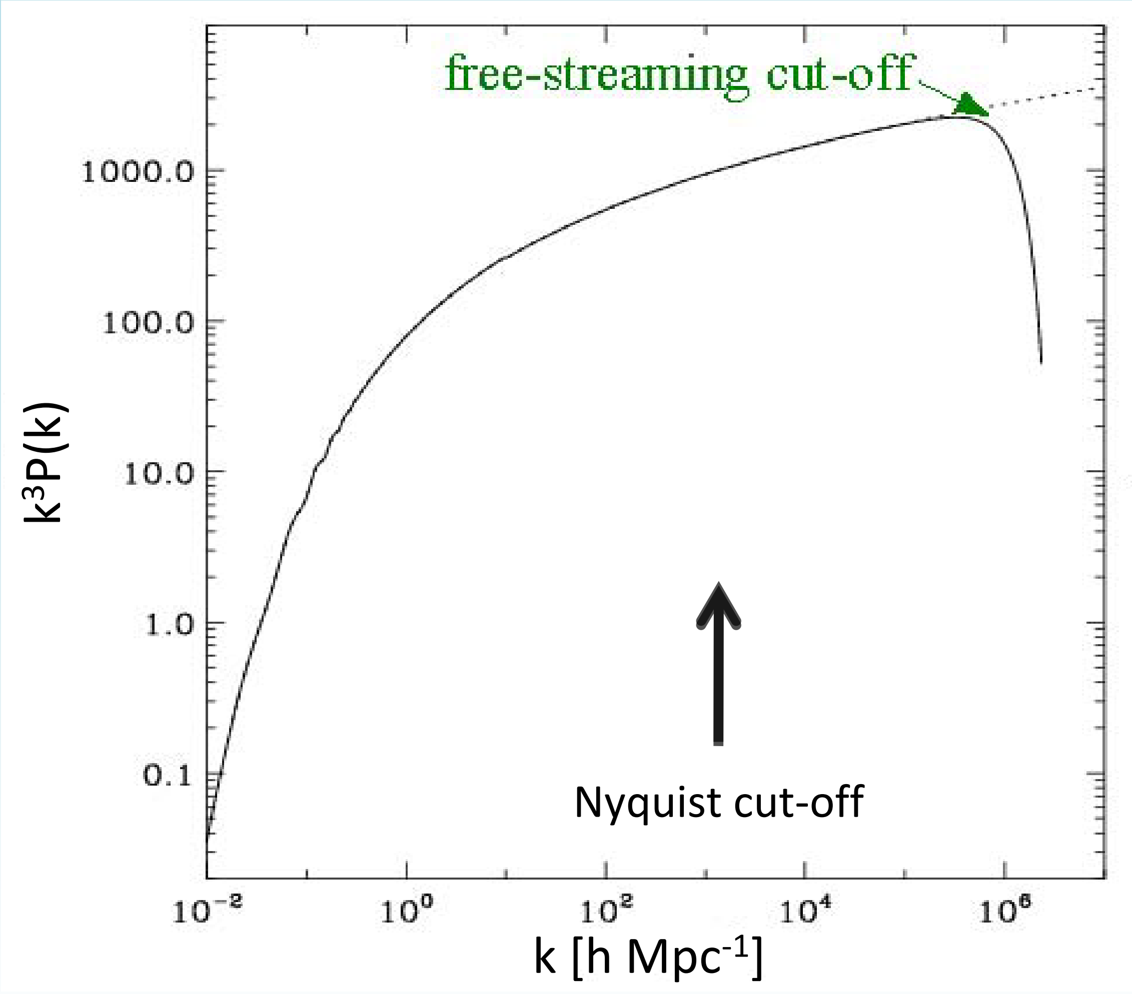

How lumpy is the MW halo?

Mass fraction in subhalos as a fn of cutoff mass in CDM PS

The Milky Way halo is expected to be quite smooth!

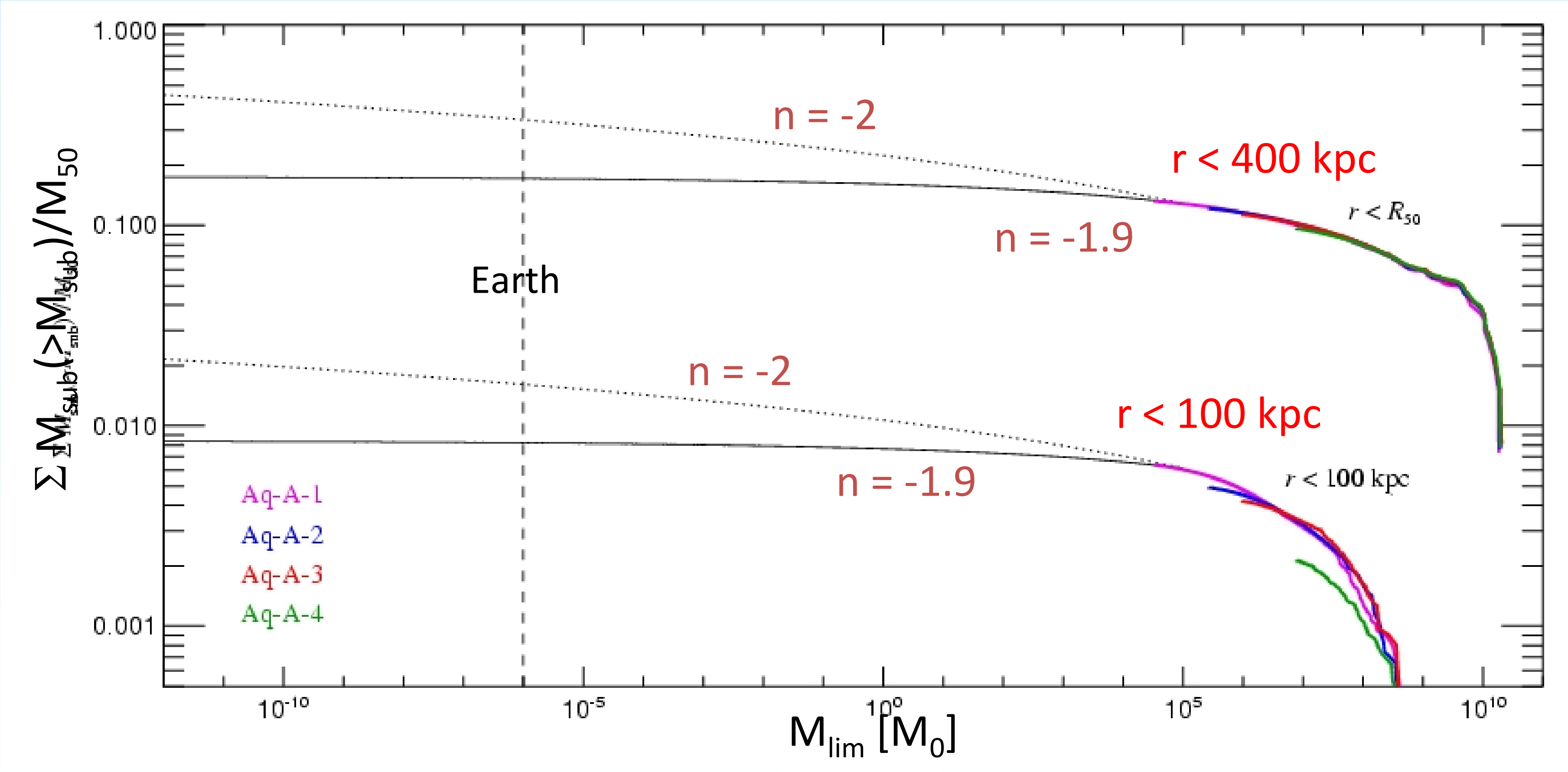

Substructure mass fraction within R_{sun} < 0.1%

Substructures within substructures

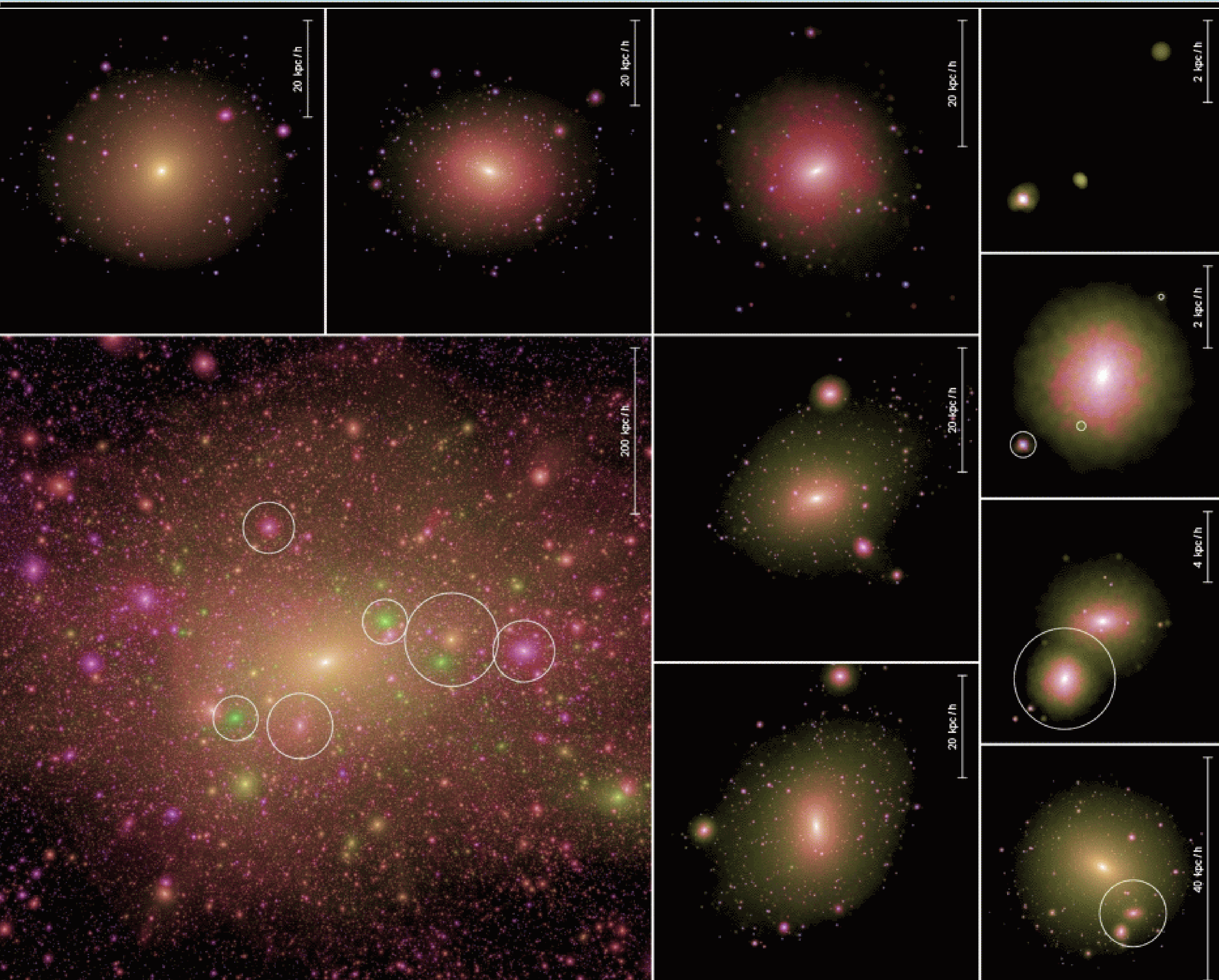

There are substructures embedded within other structures. We detect 4 generations

The hierarchy is NOT self-similar and is heavily dependent on the degree of tidal stripping of subhalos.

dependent on the degree of

Substructures within substructures

No of (sub-)substructures

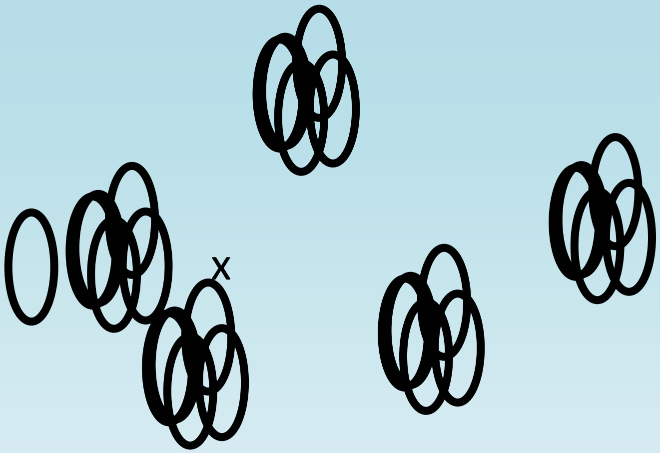

Self-similar expectation assumes subhalos are scaled down copies of main halo (corrected for resolution)

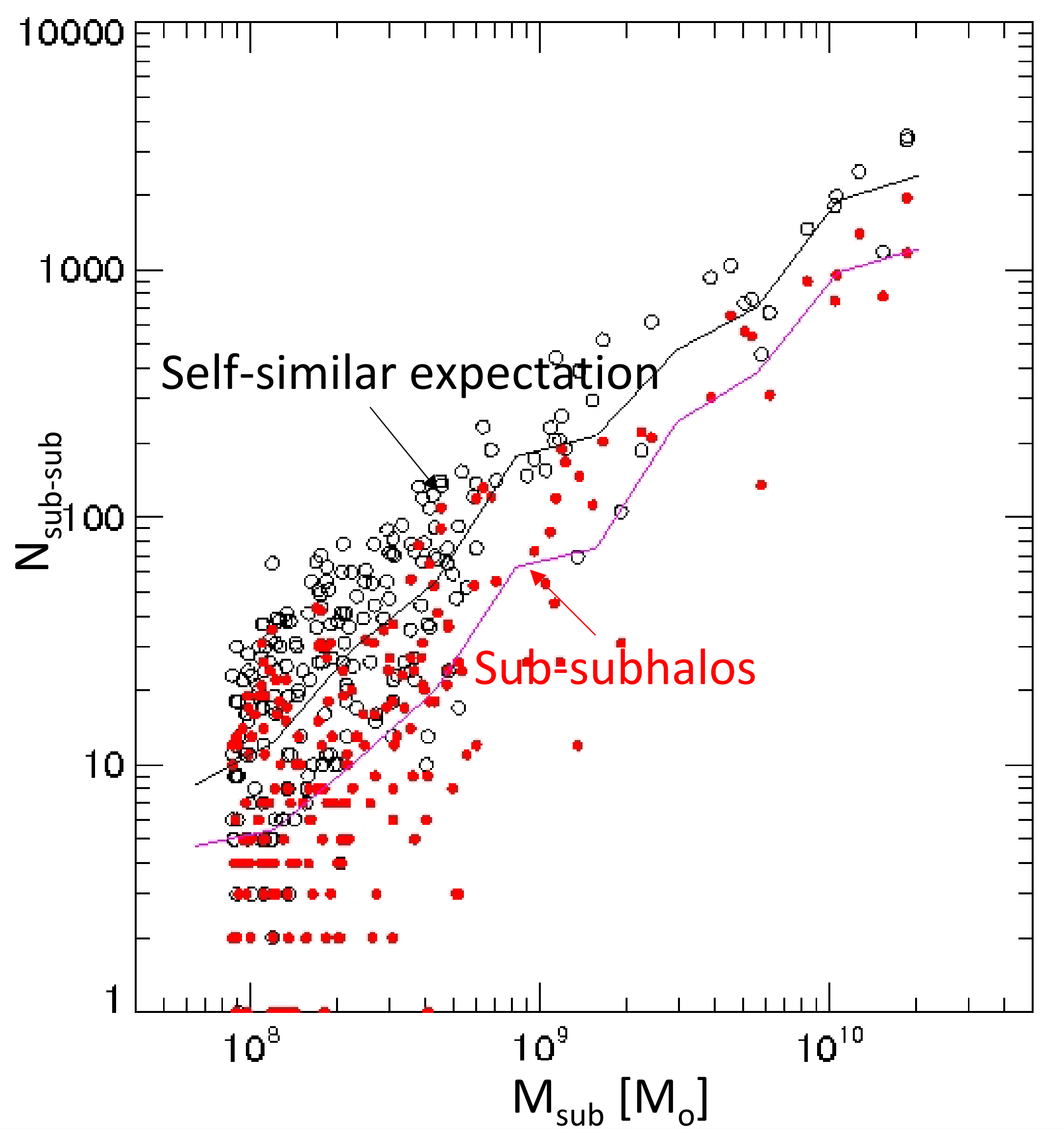

Springel et al '08

A blueprint for detecting halo CDM

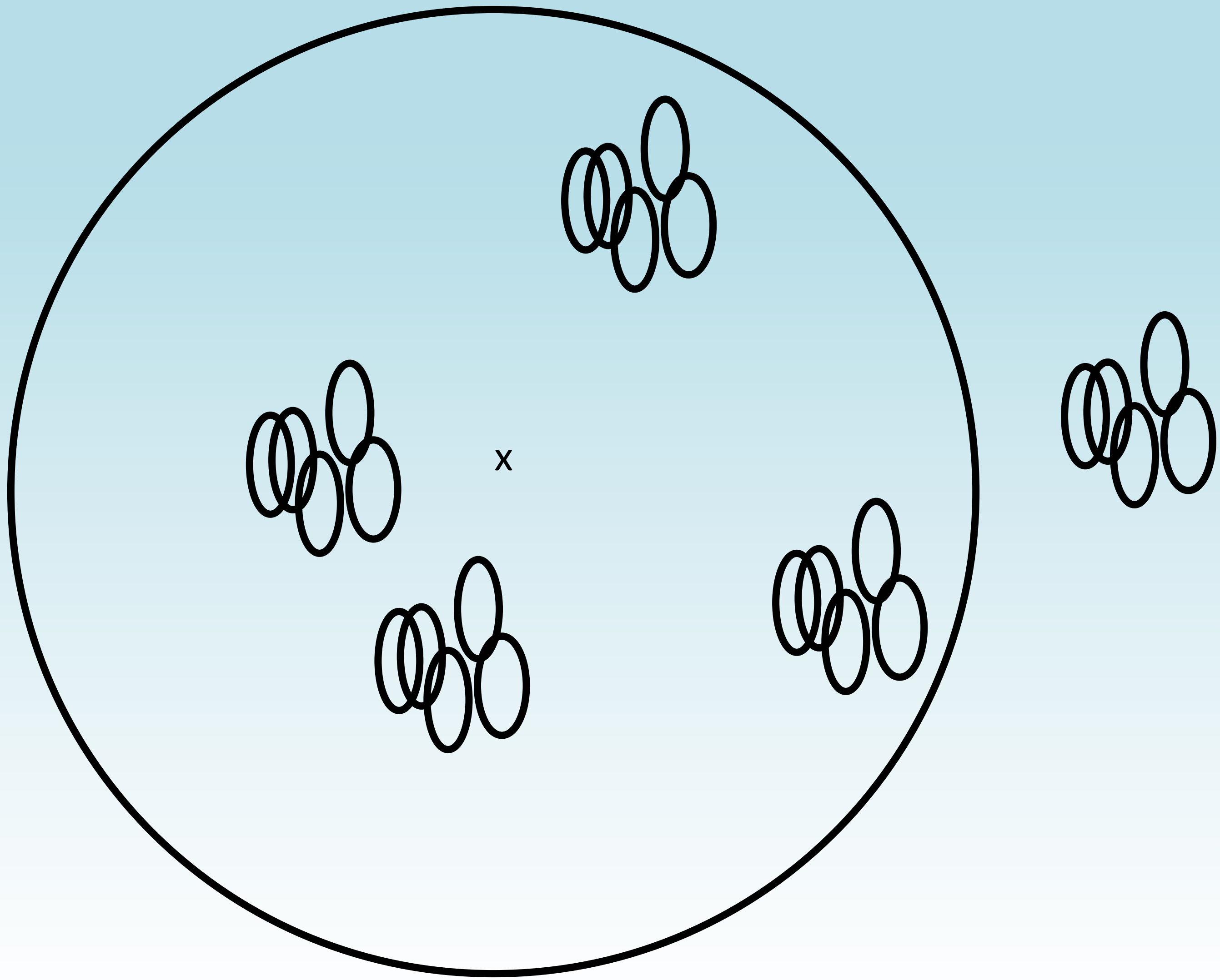

A blueprint for detecting halo CDM

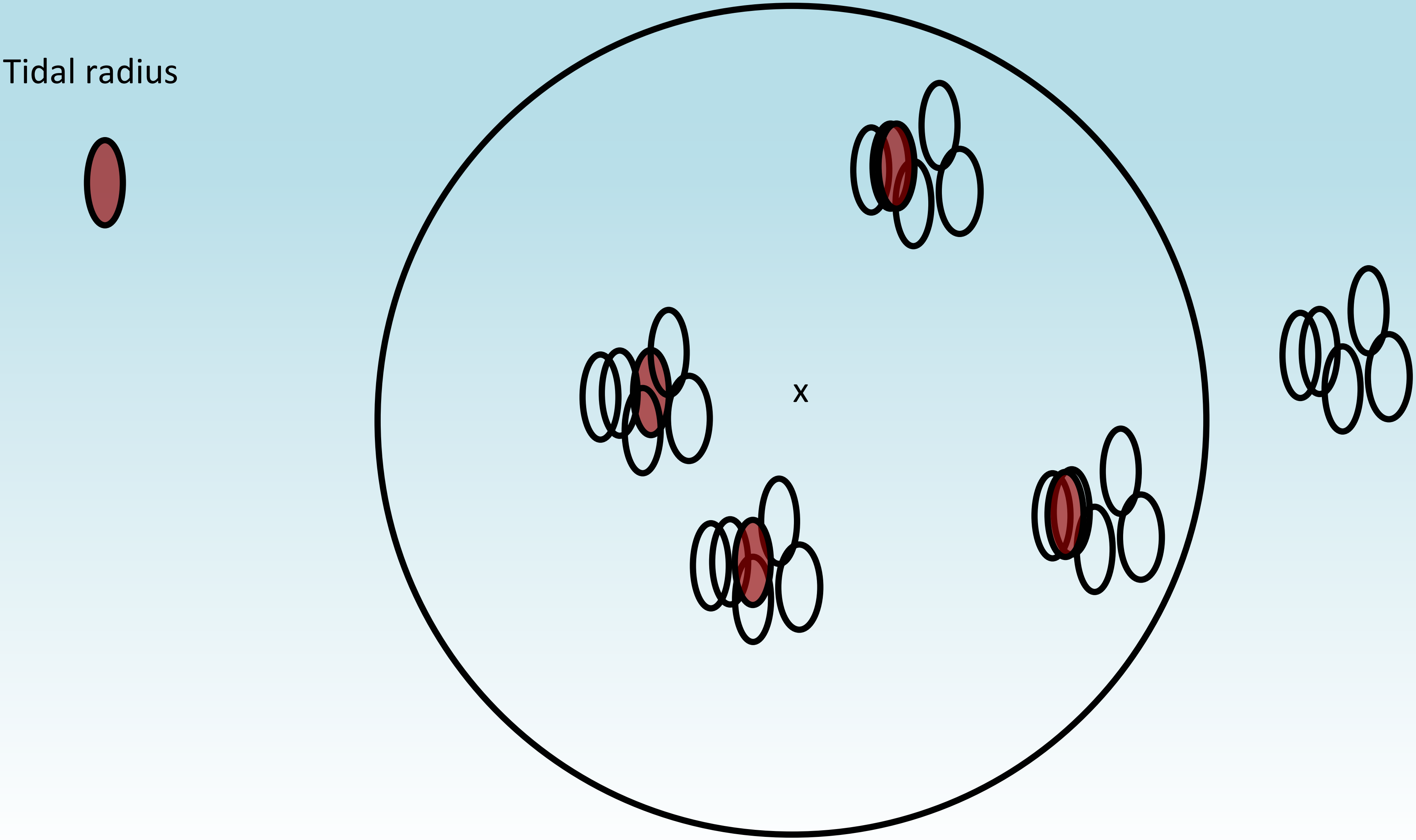

Substructures within substructures

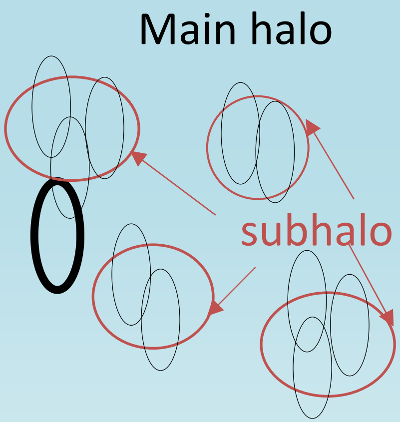

Sub-substructure abundance in subhalos is NOT, in general, a scaled-down version of that in the main halo

because:

(i) substructure abundance reduced by tidal truncation
(ii)sub-subs continue to loose mass through tides
sub-subs not replenished by infall of fresh halos

$\Longrightarrow$ Distribution of sub-substructure is NOT self-similar

A blueprint for detecting halo CDM

Supersymmetric particles annihilate and lead to production of γ-rays which may be observable by GLAST/Fermi

Intensity of annihilation radiation at *x* depends on:

$$L \propto \int \rho^2(\boldsymbol{x}) \langle \sigma v \rangle \, dV$$

halo density at ***x***

cross-section

Converges for $\rho(r)$ with slope shallower than -1.5

For NFW: $\begin{cases} 95\% \text{ of L from } r_{max} \\ 50\% \text{ of L from } 0.1 r_{max} \end{cases}$

For a smooth halo:

$$L \propto \frac{V^4{}_{\max}}{r_{\max}}$$

More on substructure convergence

Convergence in the size and maximum circular velocity for
individual subhalos cross-matched between simulation pairs.

Biggest simulation gives convergent results for

$$V_{max} > 1.5 \text{ km/s}$$
$$r_{max} > 165 \text{ pc}$$

Much smaller than the halos inferred for even the faintest dwarf galaxies

Virgo Consortium 2008

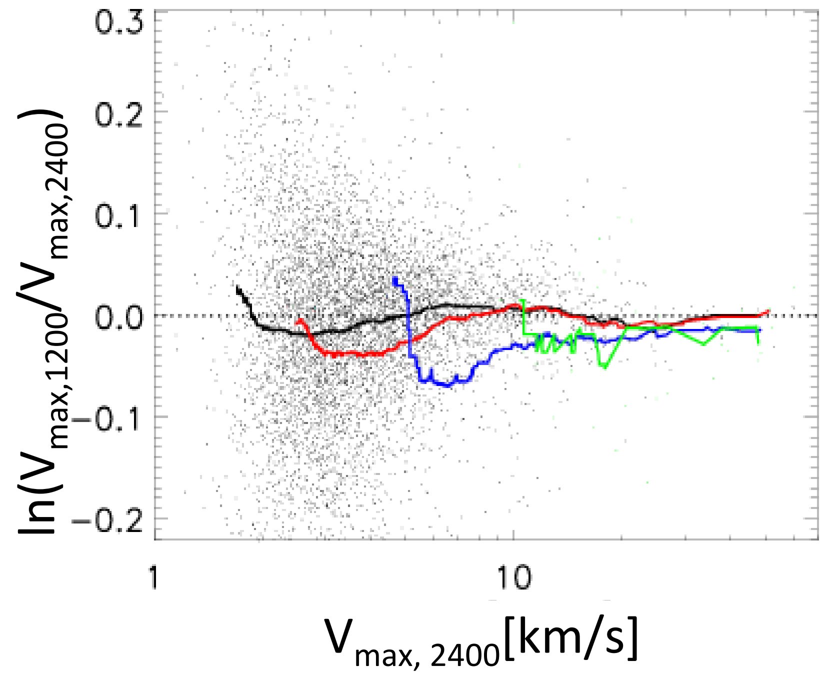

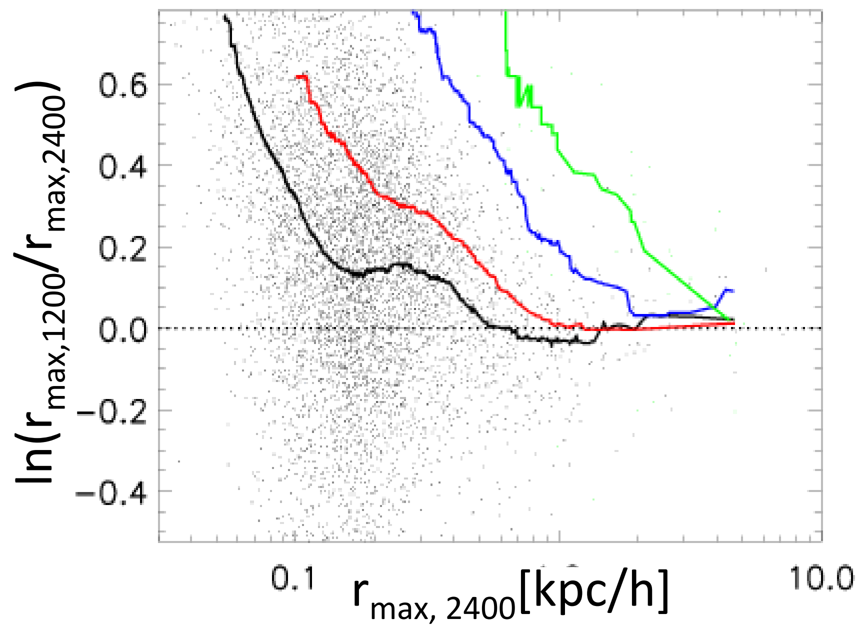

A blueprint for detecting halo CDM

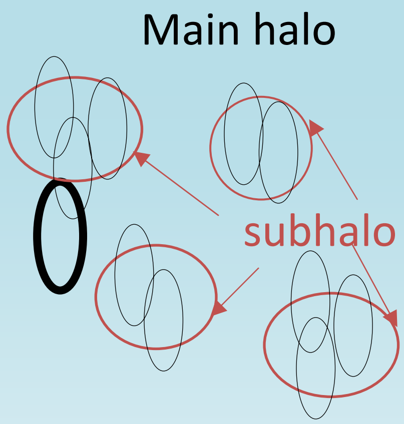

To calculate annihilation luminosity need contribution from 4 components:

1. Smooth emission from main halo
2. Smooth emission from resolved subhalos
3. Emission from unresolved subhalos in main halo
4. Emission from substructure of subhalos

Mass and annihilation radiation profiles of a MW halo

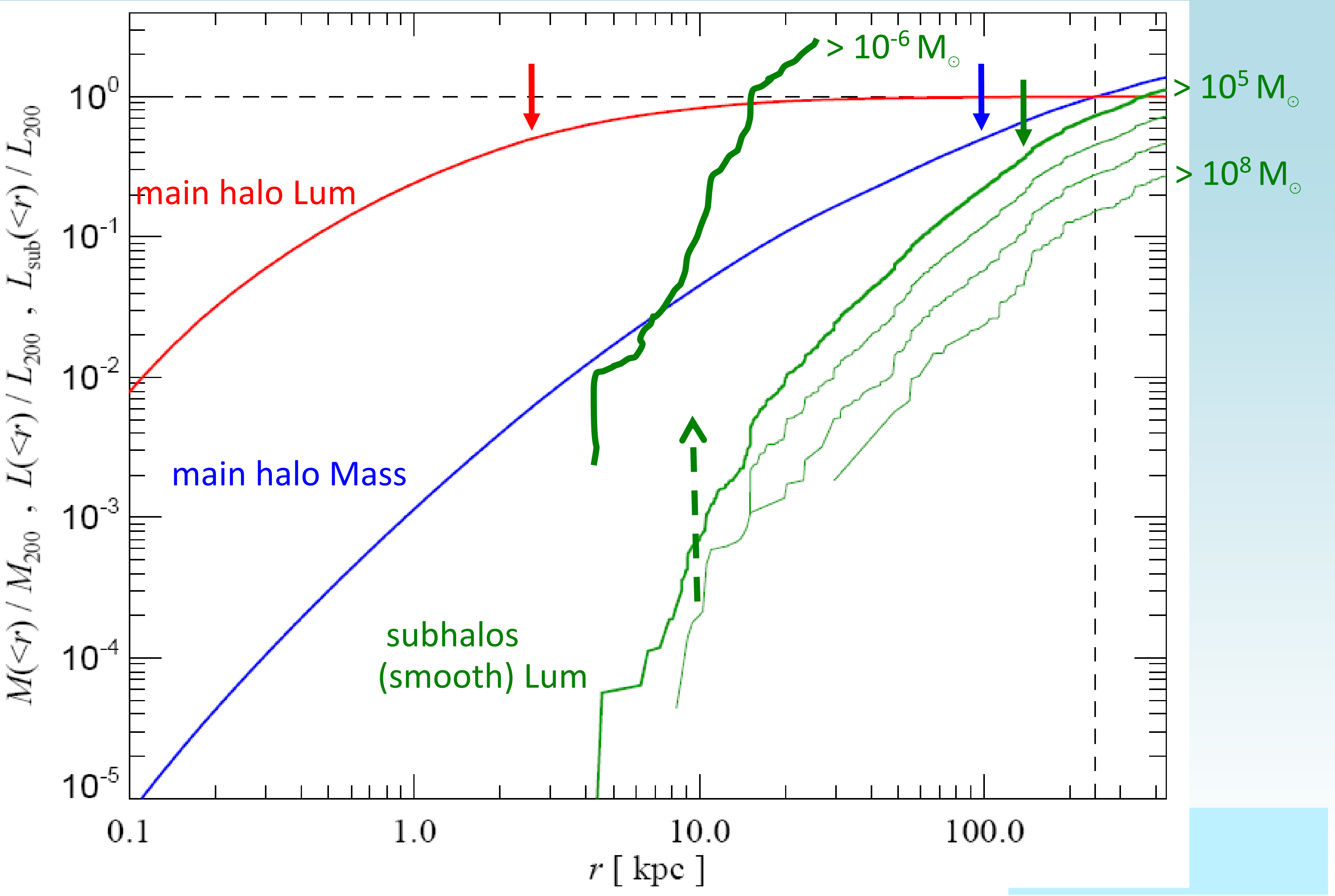

The view from outside

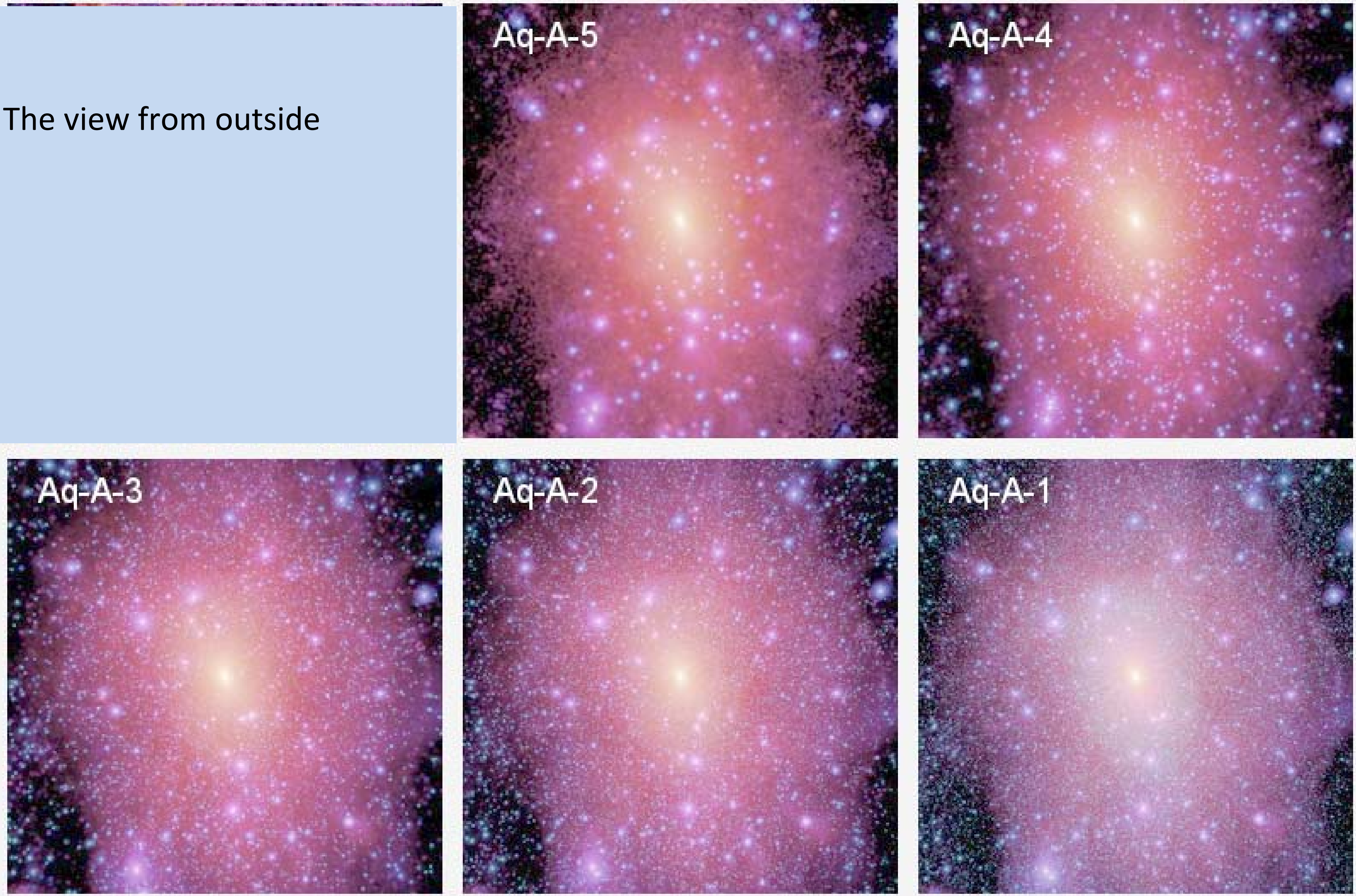

The Milky Way seen in annihilation radiation

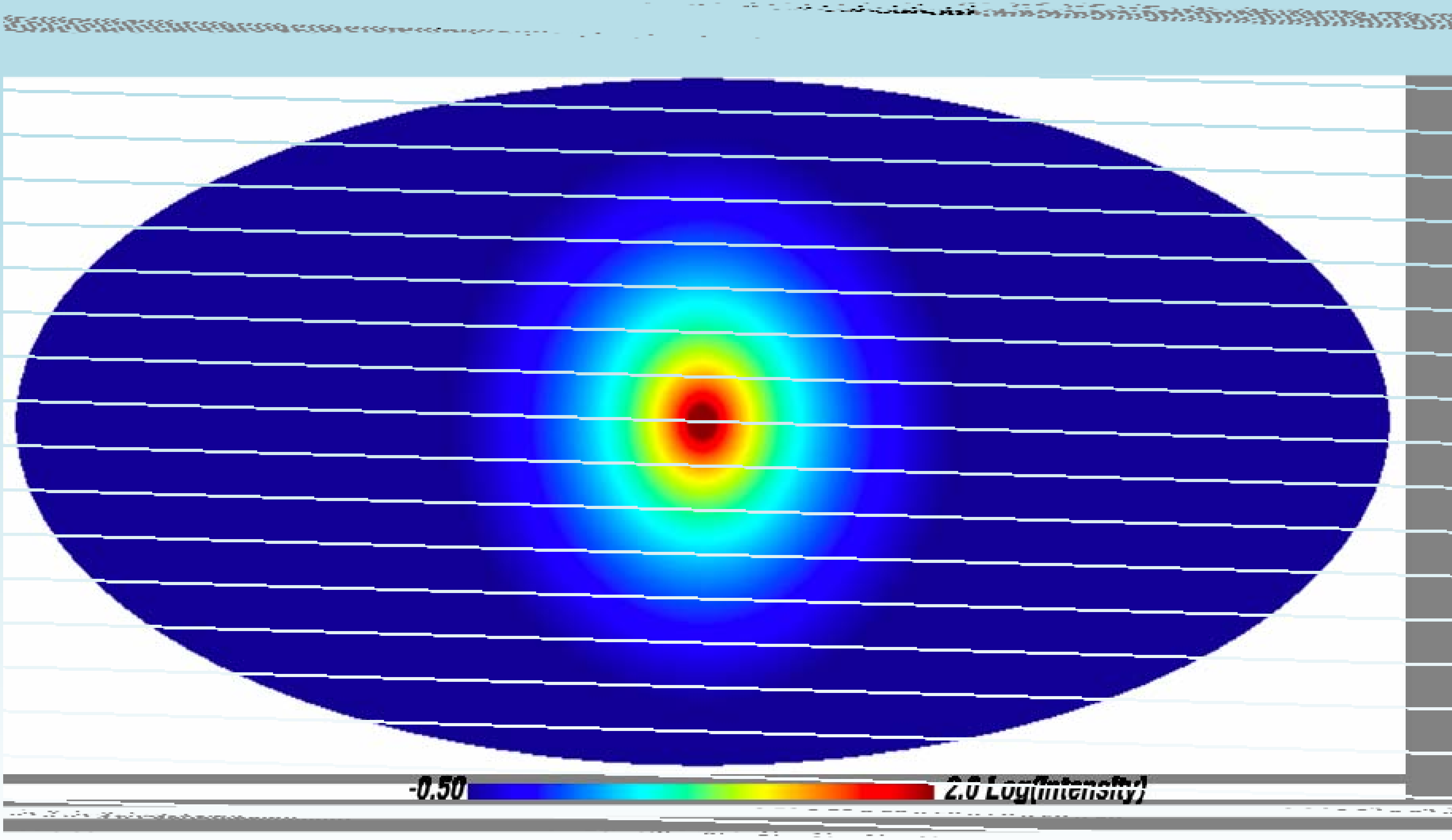

The Milky Way seen in annihilation radiation

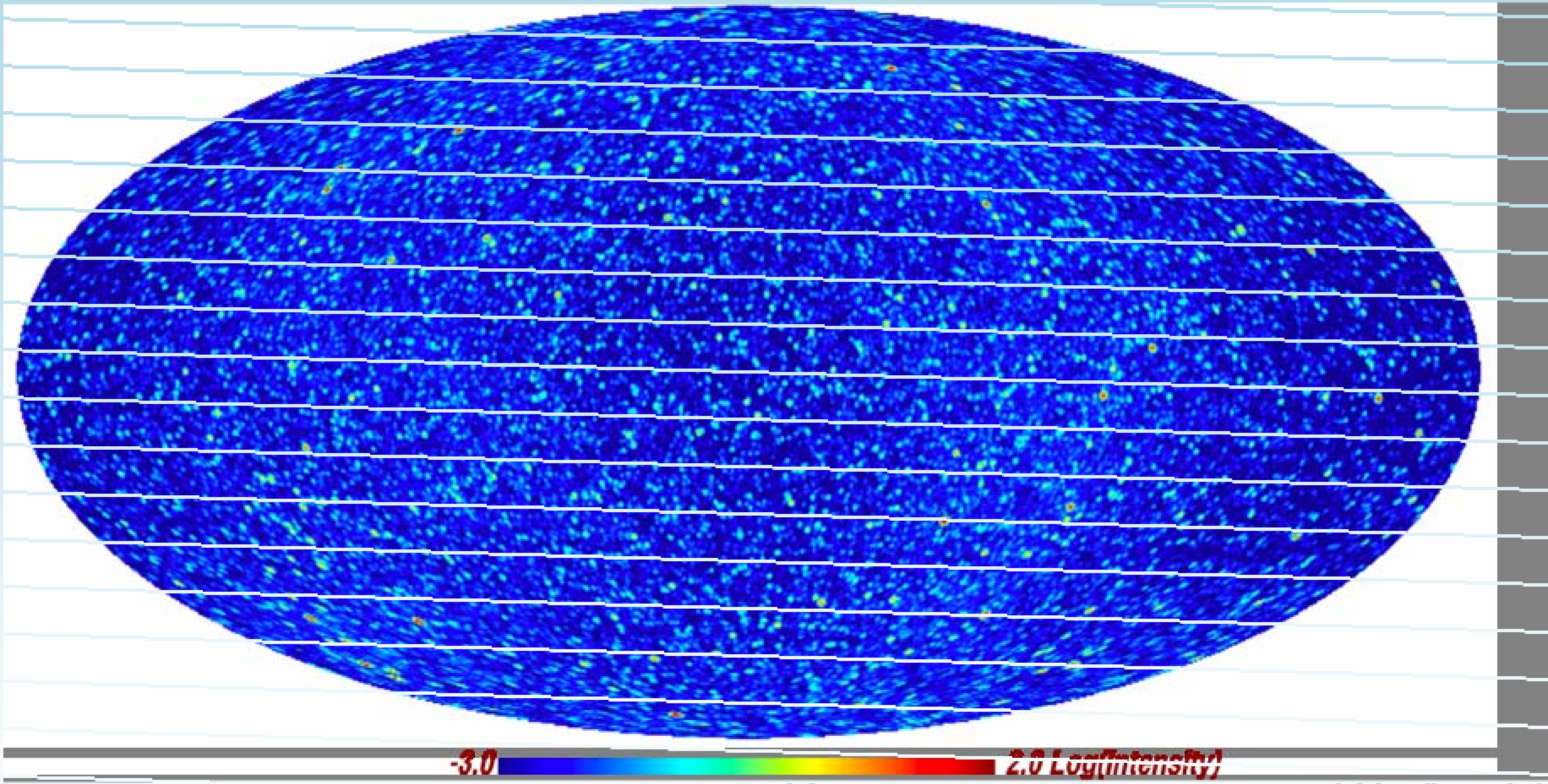

The Milky Way seen in annihilation radiation

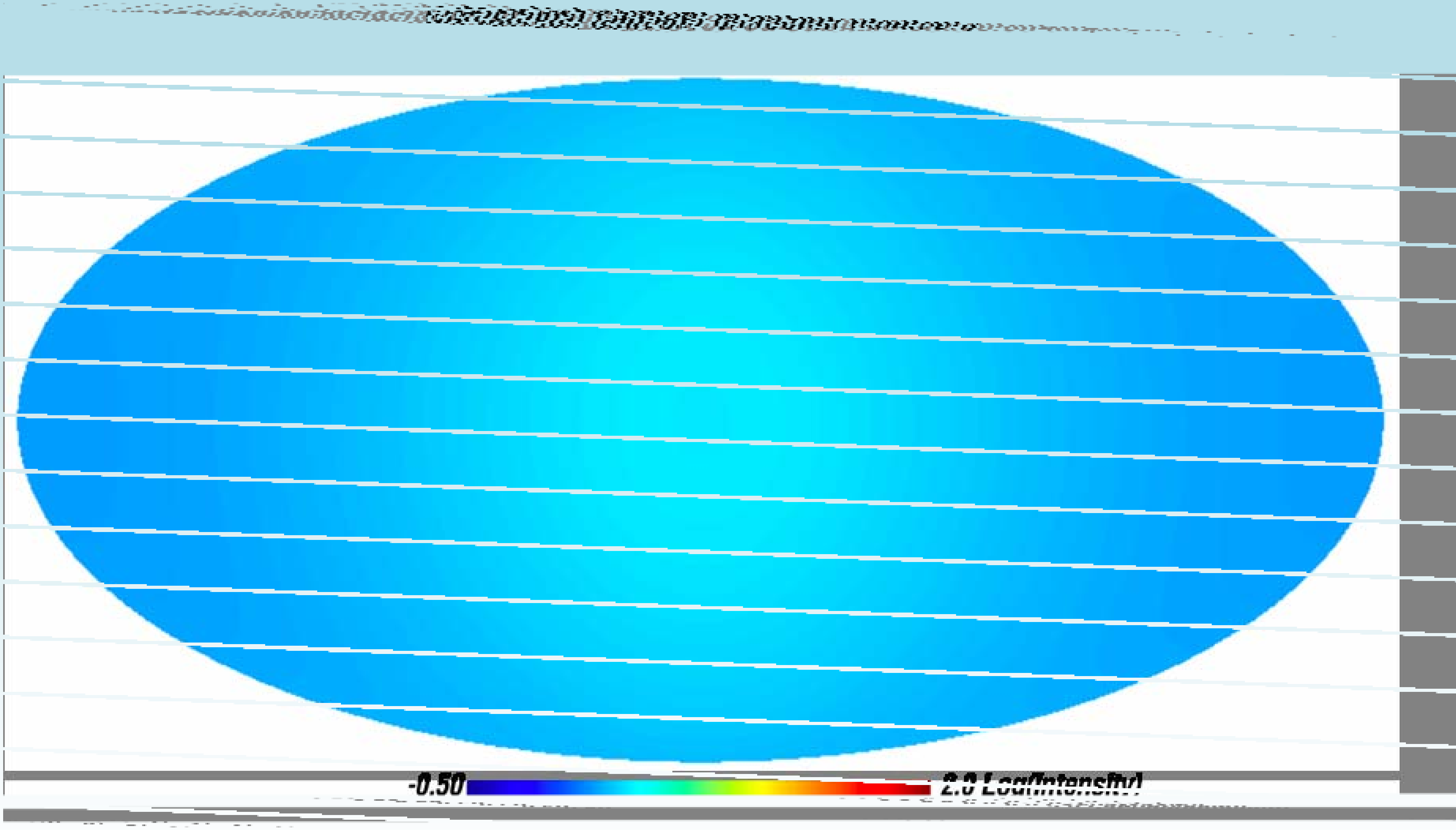

The Milky Way seen in annihilation radiation

Aquarius simulation: $N_{200} = 1.1 \times 10^9$

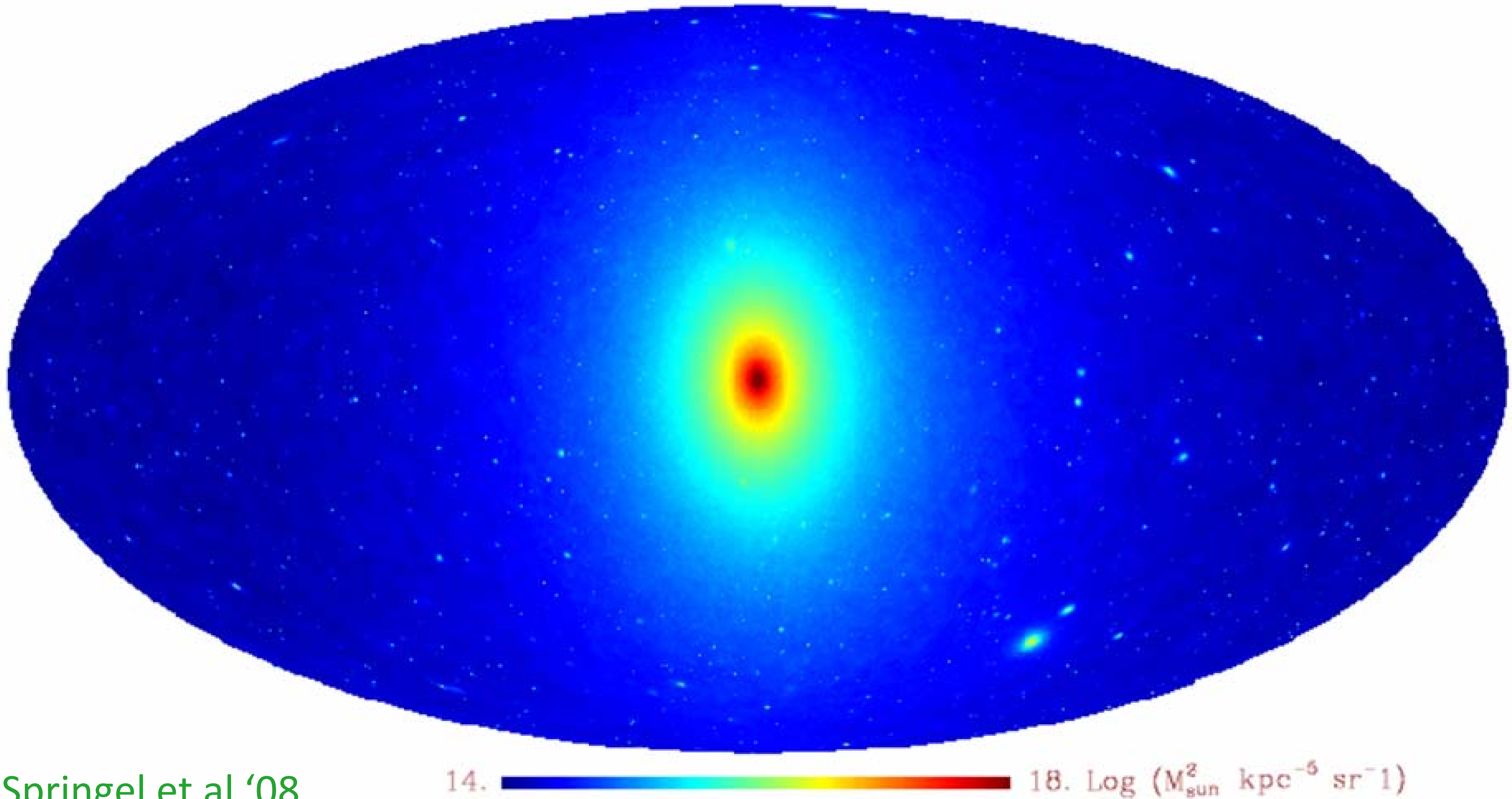

Springel et al '08

A blueprint for detecting halo CDM

$S/N = F/(\theta^2_h + \theta^2_{psf})^{1/2}$

S/N for detecting subhalos in units of that for detecting the main halo.

30 highest S/N objects, assuming use of optimal filters

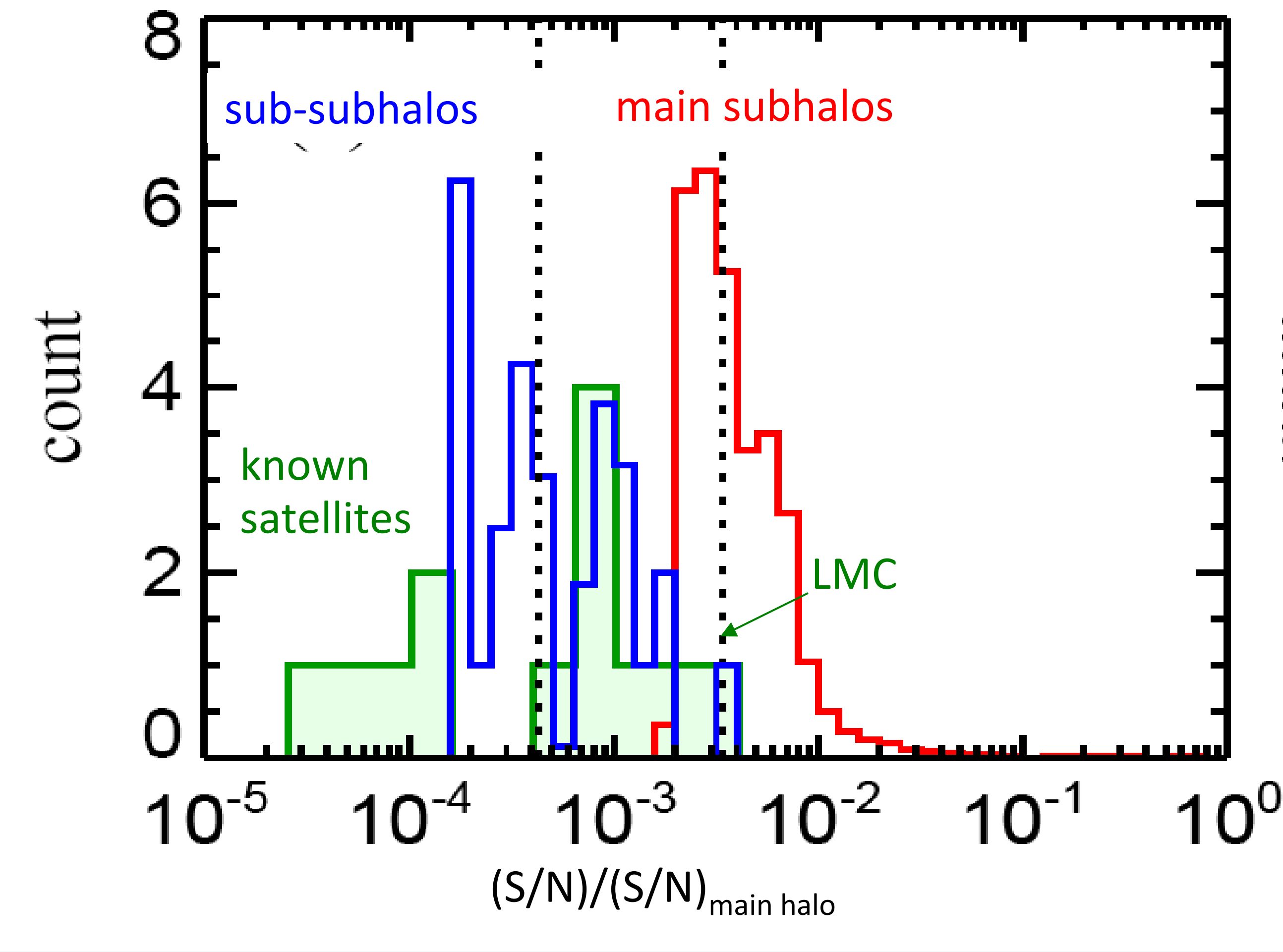

Conclusions

- Highest S/N subhalos have 1% of S/N of main halo
- Highest S/N subhalos have 10 times S/N of known satellites
- Substructure of subhalos has no influence on detectability

Talk plan

- Introduction: Structure Formation in ΛCDM Universes
- The internal structure of dark matter halos
- Predictions for annihilation radiation
- Phase space structure in the local dark matter distribution
- Summary

The cold dark matter model

Detecting cold dark matter

If CDM is a supersymmetric particle, 3 possibilities

Indirect detection through annihilation radiation (e.g. γ rays)
Direct detection (underground labs)
From evidence for SUSY at LHC

If CDM is an axion:

Direct detection in resonant cavity

The cold dark matter model

Detecting cold dark matter

If CDM is a supersymmetric particle, 3 possibilities

Indirect detection through annihilation radiation (e.g. γ rays)

Direct detection (underground labs)

From evidence for SUSY at LHC

If CDM is an axion:

Direct detection in resonant cavity

Cold dark matter searches

- Direct detection -

WIMP searches: nuclear recoil events

Axion searches: axion-photon conversion

Usually assumed astrophysical input:

Standard Halo Model (SHM):

- Smooth mass distribution
- Smooth velocity distribution
- "Featureless" phase-space

Density: ~0.3 GeV / c^2 / cm^3

Velocity: Maxwellian

Non-standard halo models

N-body simulations predict lots of phase-space substructure

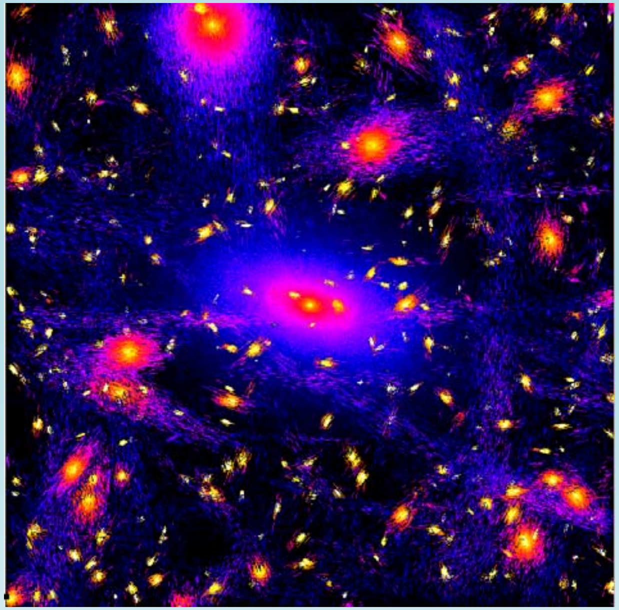

Diemand et al, Nature (2008)

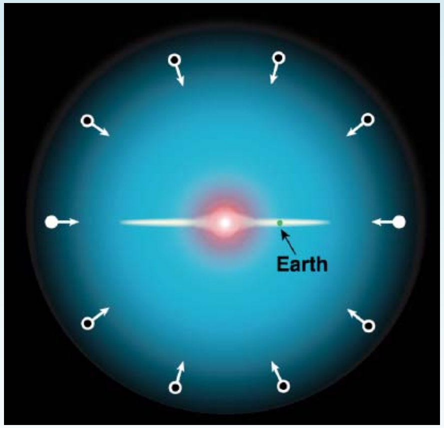

Analytic models: caustic ring model

massive streams

Van Bibber, IDM (2008)

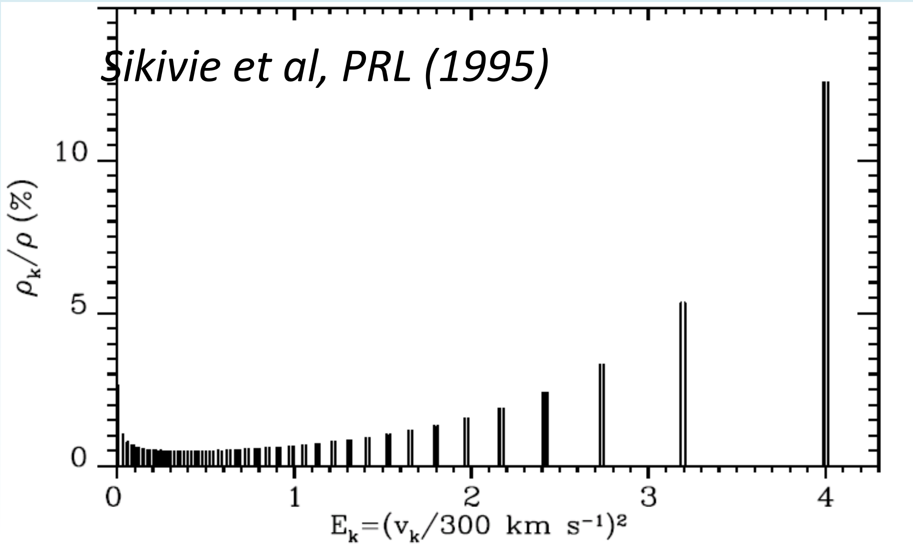

Cold dark matter searches - 3 questions -

Q1: How smooth is the dark matter mass distribution at the solar position?

Q2: How smooth is the dark matter velocity distribution at the solar position?

Q3: Does the halo formation process leave "observable" imprints?

CDM distribution around the Sun

Estimate ρ at a point by adaptive smoothing with 64 nearest particles

Fit to smooth ρ profile stratified on ellipsoids

Density prob distribution fn around solar circle

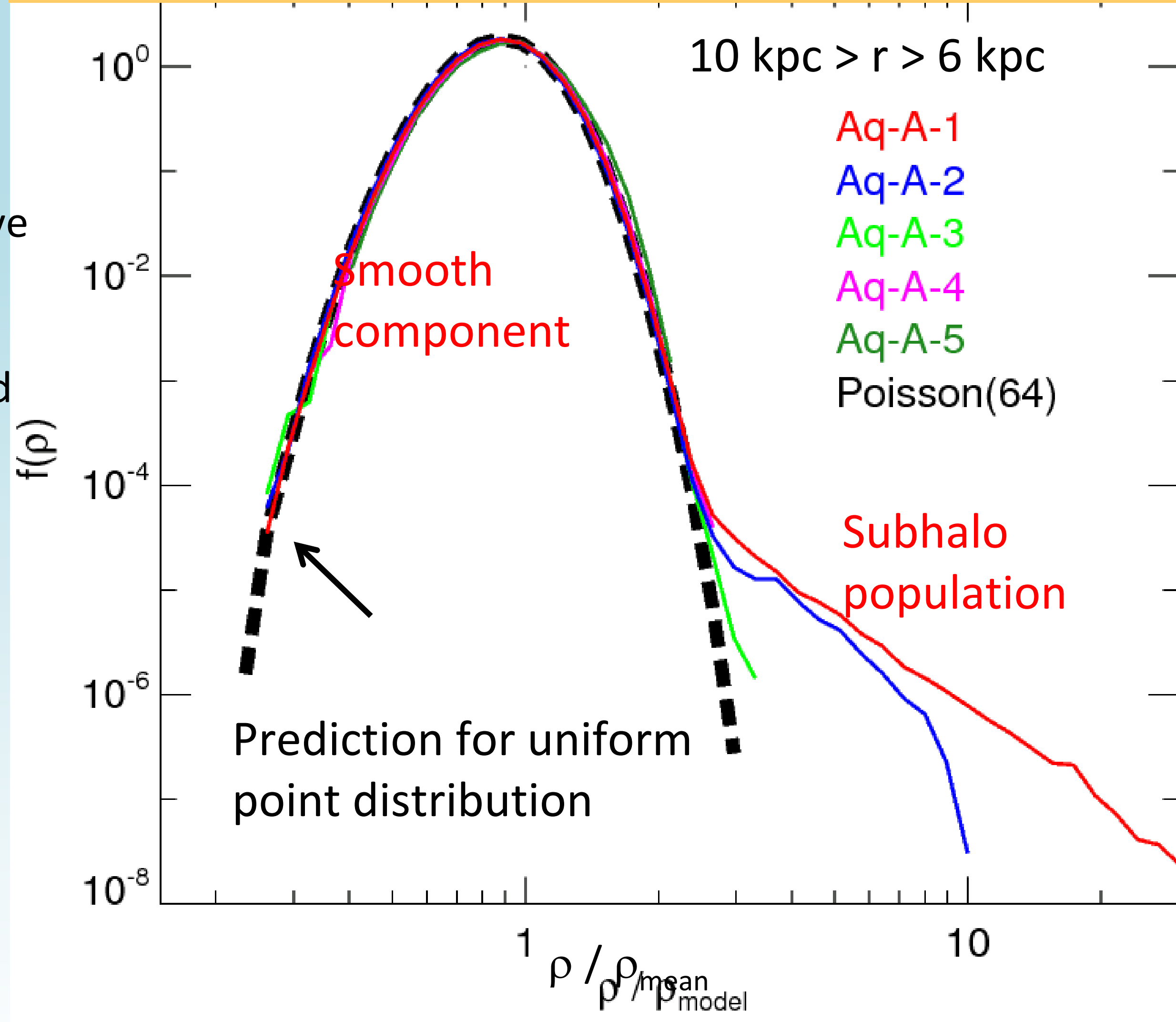

Vogelsberger et al '09

CDM distribution around the Sun

The chance of a random point lying in a substructure is $< 10^{-4}$

The *rms scatter about smooth* model for the remaining points is ~4%

Density prob distribution fn around solar circle

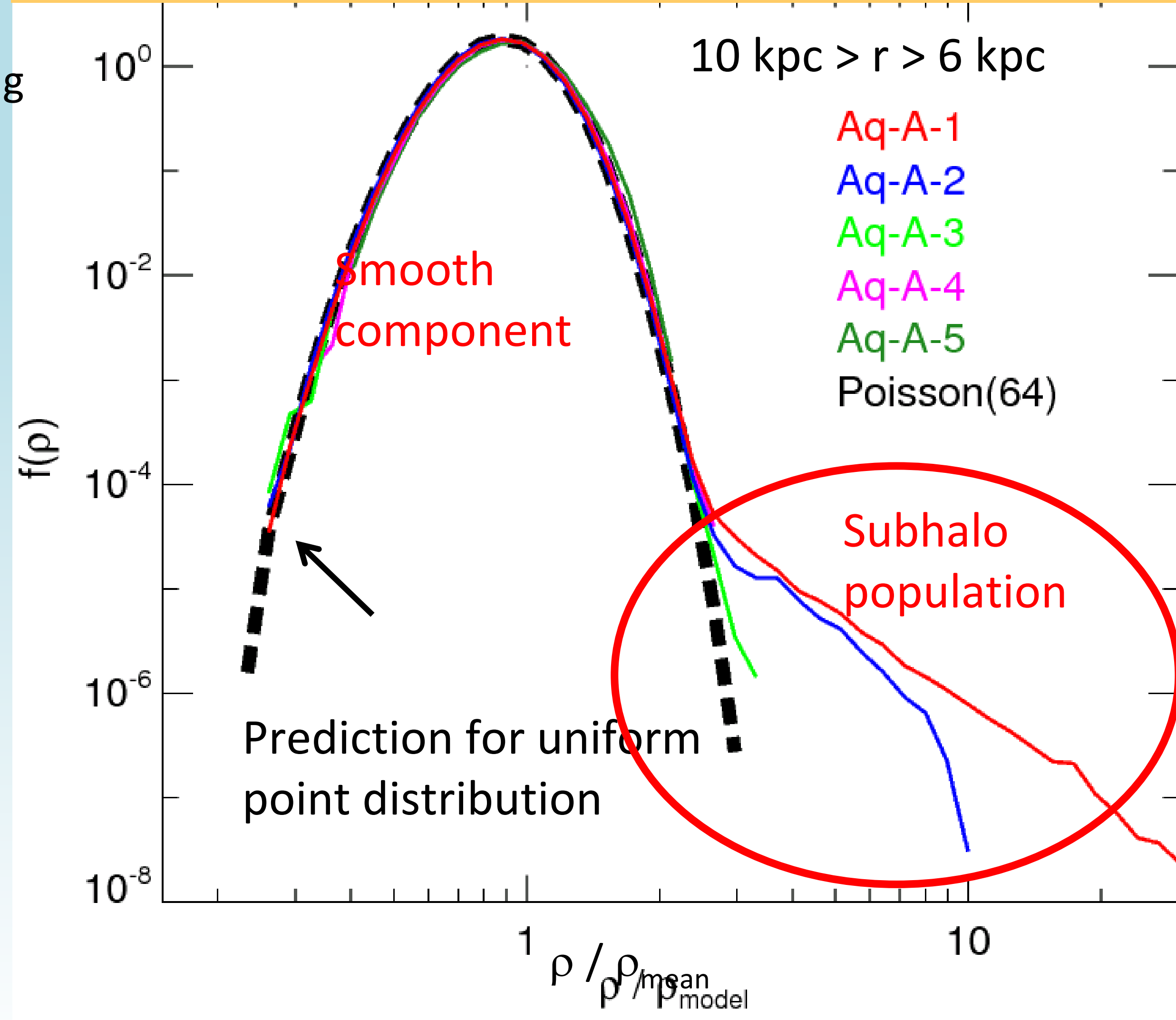

Vogelsberger et al '09

Local velocity distribution

Velocity distribution in a 2kpc box at solar circle

- Velocity histograms for particles in a typical (2kpc)^3 box at R = 8 kpc
- Distributions are smooth, near-Gaussian, and different in different directions
- No individual streams are visible

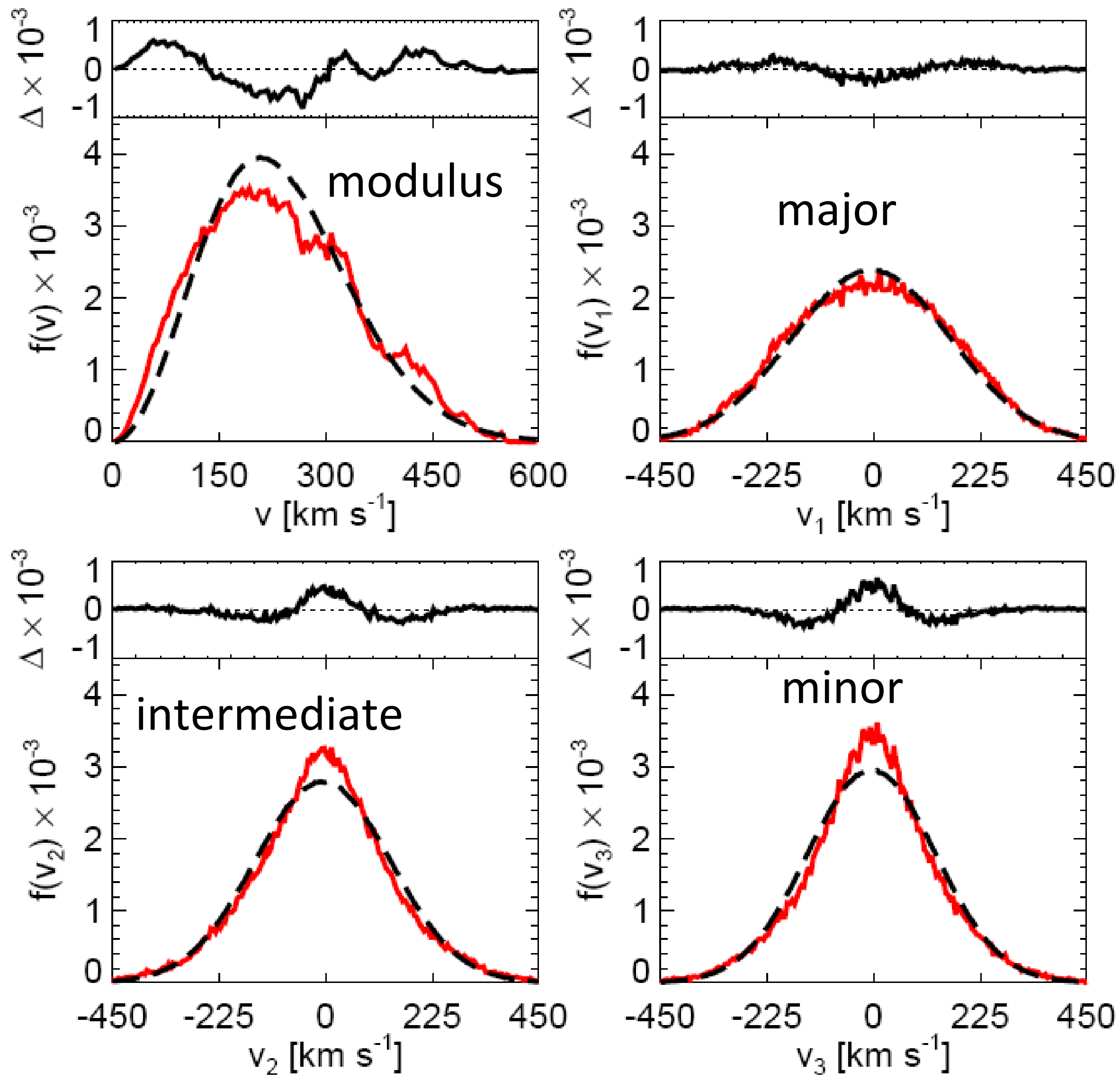

simulation

Best-fit multivariate Gaussian

Energy space features - fossils of formation

$$f(E) = \frac{\mathrm{d}M}{\mathrm{d}E}\,\frac{1}{g(E)}$$

Density of states

The energy distr. in (2 kpc)³ boxes shows bumps which:

– repeat from box to box

– stable over Gyr timescale

– different for different halos

These are potentially observable fossils of the formation process

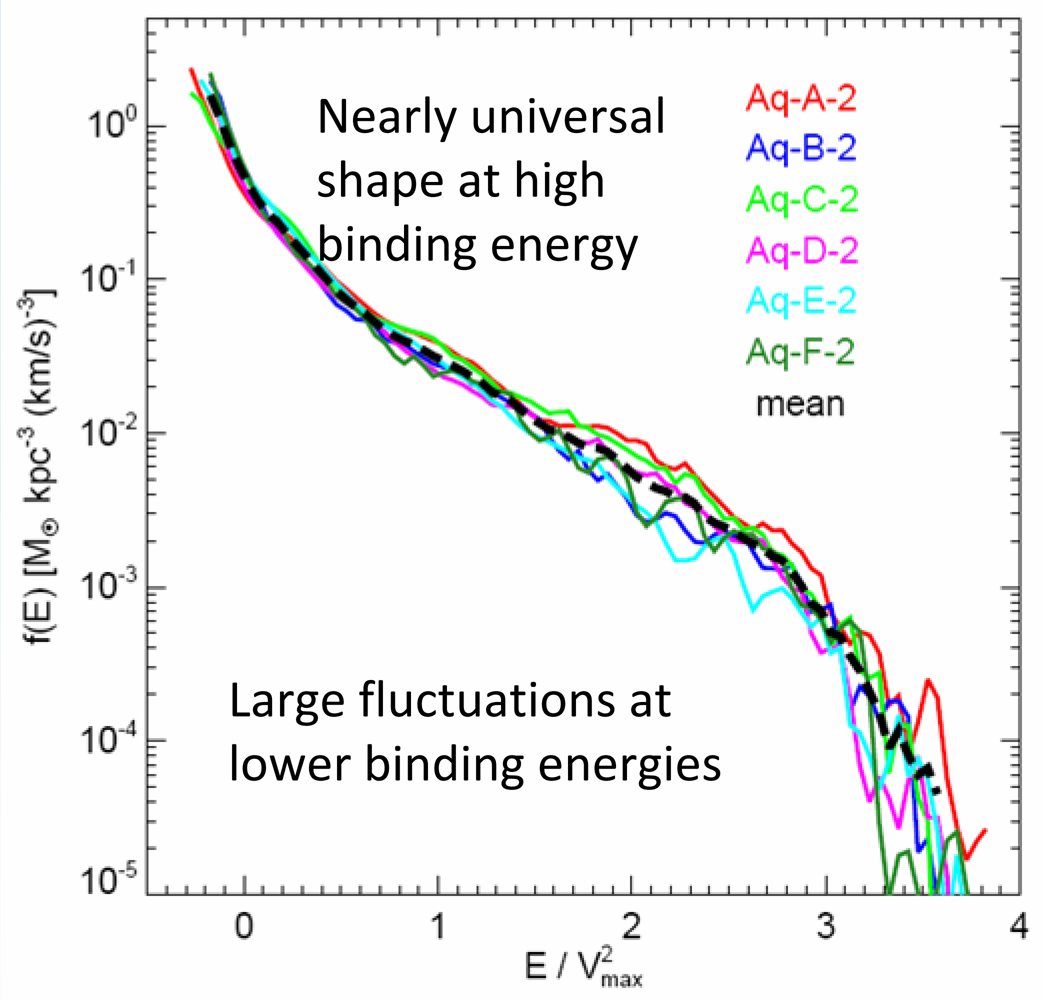

Vogelsberger et al ‘09

Effect on detector signals

Differences relative to multivariate Gaussian

WIMP recoil spectrum

Axion microwave spectrum

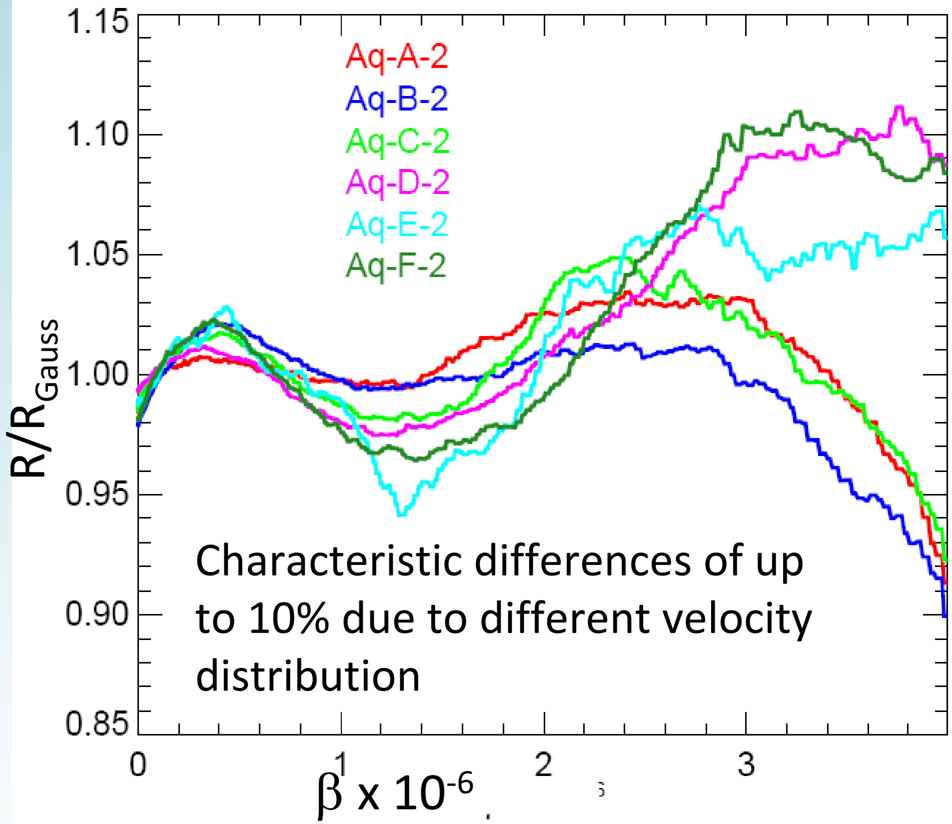

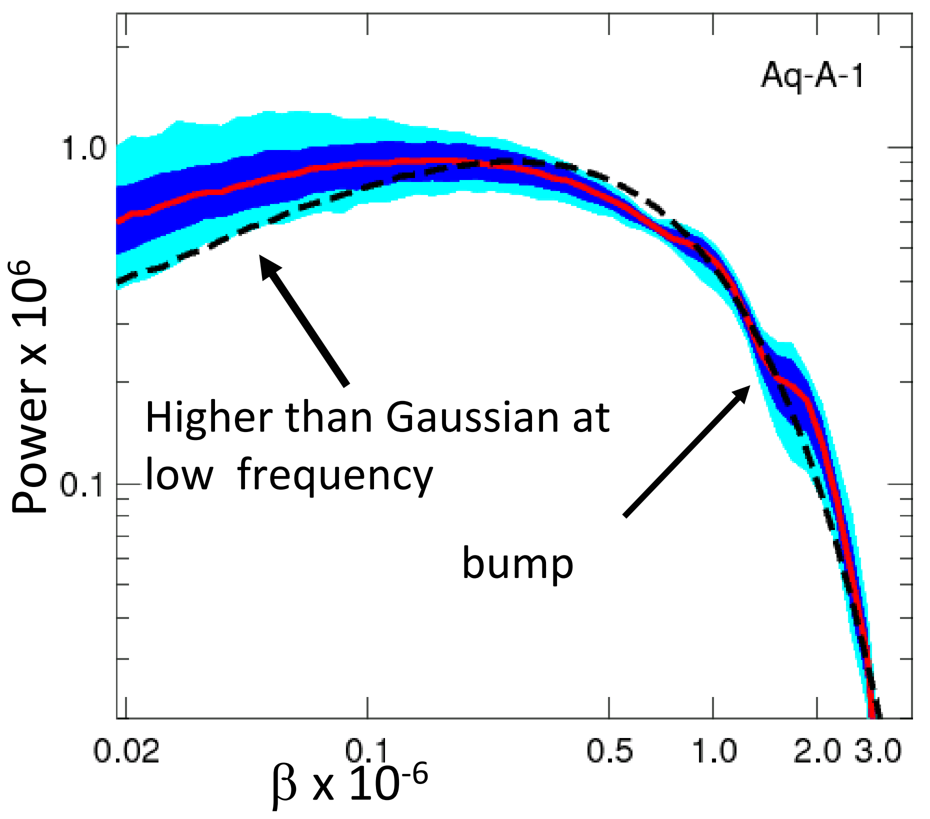

β=(v/c)

Conclusions for direct detection experiments

With more than 99.9% confidence the Sun lies in a region where the DM density differs from the smooth mean value by < 15%

The local velocity distribution of DM particles is similar to a trivariate Gaussian with no measurable “lumpiness” due to individual DM streams

The energy distribution of DM particles should contain broad features with ~10% amplitude which are the fossils of the detailed assembly history of the Milky Way's dark halo

Summary and Conclusions

- Simulations of dark matter halos can be used to aid predictions for the ΛCDM model for annihilation radiation and direct detection methods which could potentially provide confirmation of the model.

- From the solar position the main halo is the dominant signal in annihilation radiation. Substructures are harder to detect and the ones with highest signal to noise are likely to be relatively close and not the known satellites.

- At the solar circle the dark matter velocity distribution is well described by a multivariate gaussian distribution but there are features at 10% level some of which depend on the formation history of the halo.

All most certainly baryons will make a difference to the detailed predictions. The dark matter-only simulations establish a baseline for future work.

Making the initial conditions